

Binghamton University

## The Open Repository @ Binghamton (The ORB)

---

Undergraduate Honors Theses

Dissertations, Theses and Capstones

---

Spring 2022

### GlyPro as a self-immolative spacer for the release of payloads from antibody-drug conjugates

Justin Michael Howe

*Binghamton University--SUNY*, [jhowe4@binghamton.edu](mailto:jhowe4@binghamton.edu)

Follow this and additional works at: [https://orb.binghamton.edu/undergrad\\_honors\\_theses](https://orb.binghamton.edu/undergrad_honors_theses)



Part of the [Biochemistry Commons](#)

---

#### Recommended Citation

Howe, Justin Michael, "GlyPro as a self-immolative spacer for the release of payloads from antibody-drug conjugates" (2022). *Undergraduate Honors Theses*. 16.

[https://orb.binghamton.edu/undergrad\\_honors\\_theses/16](https://orb.binghamton.edu/undergrad_honors_theses/16)

This Thesis is brought to you for free and open access by the Dissertations, Theses and Capstones at The Open Repository @ Binghamton (The ORB). It has been accepted for inclusion in Undergraduate Honors Theses by an authorized administrator of The Open Repository @ Binghamton (The ORB). For more information, please contact [ORB@binghamton.edu](mailto:ORB@binghamton.edu).

GLYPRO AS A SELF-IMMOLATIVE SPACER FOR THE  
RELEASE OF PAYLOADS FROM ANTIBODY-DRUG  
CONJUGATES

BY

JUSTIN MICHAEL HOWE

THESIS

Submitted in partial fulfillment of the requirement for  
Honors Thesis in Biochemistry  
In Harpur College of Arts and Sciences of  
Binghamton University  
State University of New York  
2022

© Copyright by Justin Michael Howe 2022  
All Rights Reserved

Accepted in partial fulfillment of the requirement for  
Honors Thesis in Biochemistry  
In Harpur College of Arts and Sciences of  
Binghamton University  
State University of New York  
2022

Dr. L. Nathan Tumey, Faculty Advisor  
Department of Pharmacy and Pharmaceutical Sciences, Binghamton University

Dr. Christof T. Grewer, Member  
Department of Chemistry, Binghamton University

Dr. Ming An, Member  
Department of Chemistry, Binghamton University

## **Abstract**

Antibody-drug conjugates (ADCs) are an increasingly popular modality for targeted drug delivery in many oncological and immunological applications. The paratope of a monoclonal antibody (mAb) directs the delivery of a conjugated therapeutic payload to antigen expressing cells, resulting in a controlled transport of payload to a desired cell type. Internalization of the ADC followed by lysosomal degradation results in the release of a payload to perform its biochemical function. A chemical linker between the drug and the antibody is responsible for the stability of the conjugate in circulation alongside mediating the release of an unmodified payload under lysosomal conditions. Currently, the lead linker, ValCit-p-aminobenzyl carbamate (PABC), has demonstrated impressive extracellular integrity while maintaining susceptibility to lysosomal proteases, such as Cathepsin B, for controlled intracellular release.<sup>1</sup> However, the well-studied ValCitPABC linker system is largely restricted to amine-containing payloads for immuno-modulating ADCs whereas there are few ADC linkage systems that are able to release alcohol containing payloads, regardless of their functional prevalence across a myriad of biologically active small molecules. We propose that upon cathepsin-mediated cleavage of our ADCs, the ValCit release of a GlyPro ester undergoes rapid cyclization to form a diketopiperazine, thereby releasing the alcohol-containing payload.

The efficiency of this linker (ValCitGlyPro) was examined using a model system designed to release dexamethasone, a potent glucocorticoid. Kinetic studies demonstrated that our linker system results in rapid GlyPro-dexamethasone release in lysosomes, which undergoes rapid cyclization to release dexamethasone at neutral pH. After conjugation of the linker payload to targeted and untargeted antibodies, several cell assays show that this system is capable of targeted immune suppression of lipopolysaccharide (LPS) stimulated

cells. We also report our efforts to expand the utility of this linker system for the release of anilines, and amines.

## Table of Contents

<i>Abstract</i> .....	<i>iv</i>
<i>List of Tables</i> .....	<i>viii</i>
<i>List of Figures</i> .....	<i>ix</i>
<i>List of Supplemental Figures</i> .....	<i>x</i>
<i>1. Introduction</i> .....	<i>1</i>
<i>1.1 Statement of Purpose</i> .....	<i>3</i>
<i>2. Simple Esterase Linkage</i> .....	<i>3</i>
<i>3. Synthesis of ValCitGlyPro Linker-payloads and ADCs</i> .....	<i>5</i>
<i>4. In Vitro ValCitGlyPro Catabolism Comparison to Non-Cleavable mc Linker</i> .....	<i>8</i>
<i>5. Functional group Evaluation for Release from ValCitGlyPro</i> .....	<i>9</i>
<i>6. Immune Activation of Ramos Blue Cells by ValCitGlyPro_resiquimod ADCs</i> .....	<i>12</i>
<i>7. Immune Suppression of Activated Monocytes by ValCitGlyPro_dex ADCs</i> .....	<i>13</i>
<i>8. Dose Response of anti-TNF<math>\alpha</math> ADCs containing mpValCitGlyPro_dex</i> .....	<i>16</i>
<i>9. Discussion and Conclusions</i> .....	<i>18</i>
<i>10. Experimental Methods</i> .....	<i>21</i>
<i>10.1 Organic Synthesis of mpValCitGlyPro_dexamethasone</i> .....	<i>21</i>
<i>10.2 Organic Synthesis of mcValCitGlyPro_resiquimod</i> .....	<i>22</i>
<i>10.3 Organic Synthesis of mcValCitGlyPro_doxorubicin</i> .....	<i>24</i>

<i>10.4 Organic Synthesis of mcValCitGlyPro_dexamethasone</i> .....	26
<i>10.5 mAb Conjugation Procedure</i> .....	27
<i>10.6 Lysosomal Catabolism, mc_dex ADCs</i> .....	28
<i>10.7 lysosomal Catabolism, mc_dex vs mpValCitGlyPro_dex ADCs</i> .....	28
<i>10.8 Lysosomal Catabolism, Linker-payload Leaving Group Ability from GlyPro</i> .....	29
<i>10.9 Ramos Blue Cell Stimulation Assay</i> .....	30
<i>10.10 THP-1 Monocyte Suppression ADC Screen</i> .....	31
<i>10.11 Normal Analytical UPLC-MS Method</i> .....	33
<i>10.12 Normal Analytical HPLC-MS Method</i> .....	34
<i>10.13 Normal Preparative HPLC Method</i> .....	34
<i>11. Supplemental Material</i> .....	36
<i>12. Acknowledgements</i> .....	43
<i>13. References</i> .....	44



## List of Tables

<i>Table 1: Solvent Gradient of Normal UPLC-MS Method</i> .....	33
<i>Table 2: Solvent Gradient for Normal Analytical HPLC-MS Method</i> .....	34
<i>Table 3: Solvent Gradient for Normal preparative HPLC Method</i> .....	35
<i>Table 4: List of ADCs, their DAR, concentration, and aggregation</i> .....	42

## List of Figures

<i>Figure 1: Mechanism of internalization of an ADC</i> <sup>24</sup> .....	1
<i>Figure 2: Release mechanism of payload* attached to mcValCitPABC linker</i> .....	2
<i>Figure 3: Catabolism of ADCs assay schematic for ester cleavage evaluation</i> .....	3
<i>Figure 4: mc_dex ADC catabolism schematic and catabolism results, need for a self-immolative linker system</i> .....	4
<i>Figure 5: The necessity of a self-immolative linker for alcohol containing payloads</i> .....	5
<i>Figure 6: Novel cleavable linker mechanism for the release of alcohol-containing payloads, such as dexamethasone</i> .....	5
<i>Figure 7: Synthesis of mcValCitGlyPro_X linker-payloads and ADCs</i> .....	7
<i>Figure 8: Catabolism schematic of mc_dex vs mcValCitGlyPro_dex ADCs</i> .....	8
<i>Figure 9: ADC containing GlyPro self-immolative linker compared to standard ester linkage for release of dexamethasone</i> .....	9
<i>Figure 10: Catabolism assay conditions of cys_mcValCitGlyPro_X linker-payloads</i> .....	11
<i>Figure 11: Release of payloads from GlyPro self-immolative linker catabolism</i> .....	11
<i>Figure 12: Linker-payload catabolism and cyclization proposed mechanism for payload release</i> .....	12
<i>Figure 13: NF-<math>\kappa</math>B stimulation of Ramos Blue cells from GlyPro containing ADCs</i> .....	13

*Figure 14: TNF $\alpha$  suppression after LPS stimulation by targeted and untargeted dexamethasone ADCs* ..... 14

*Figure 15: mpValCitGlyPro\_dex ADC screen for THP-1 suppression assay, NF- $\kappa$ B (left) and IRF (right) decrease after 1ng/mL LPS stimulation* ..... 16

*Figure 16: Schematic illustration of tmTNF $\alpha$  and TACE* ..... 16

*Figure 17: THP-1 monocyte NF- $\kappa$ B suppression after 1ng/mL LPS stimulation, dose response of ValCitGlyPro\_dex ADCs with and without TACE inhibitor* ..... 18

**List of Supplemental Figures**

*Figure S 1: anti-CD11a\_mpValCitGlyPro\_dex mass spectrometry traces, linker-payload exact mass: ~953dalt* ..... 36

*Figure S 2: anti-RSV\_mpValCitGlyPro\_dex mass spectrometry traces, linker-payload exact mass: ~953dalt* ..... 36

*Figure S 3: anti-TNF $\alpha$ \_mpValCitGlyPro\_dex mass spectrometry traces, linker-payload exact mass: ~953dalt* ..... 37

*Figure S 4: LCMS Trace Characterization for mpValCitGlyPro\_dex* ..... 37

*Figure S 5: LCMS Trace Characterization for alloc\_ValCitGlyPro\_resiquimod* ..... 38

*Figure S 6: LCMS Trace Characterization for mcValCitGlyPro\_resiquimod* ..... 39

*Figure S 7:LCMS Trace Characterization for alloc\_ValCitGlyPro\_doxorubicin* ..... 39

*Figure S 8: LCMS Trace Characterization for mcValCitGlyPro\_doxorubicin ..... 40*

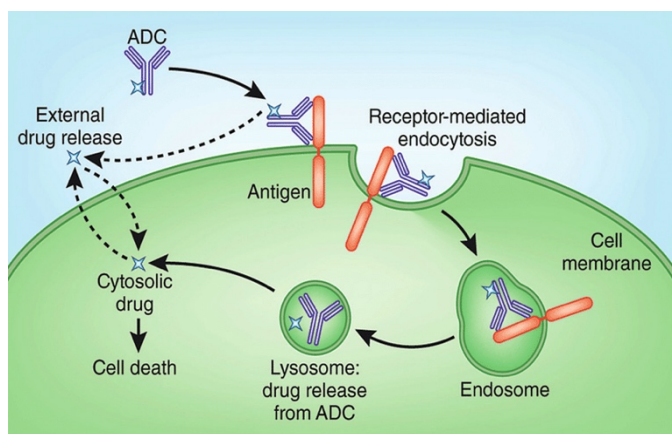
*Figure S 9: LCMS Trace Characterization for alloc\_ValCitGlyPro\_dexamethasone ..... 41*

*Figure S 10: LCMS Trace Characterization for mcValCitGlyPro\_dexamethasone ..... 42*

## 1. Introduction

Targeted-drug delivery has grown in prevalence in medicinal chemistry to bypass off target drug effects that may occur from systemic administration of a biologically active compound.<sup>2</sup> This targeted-drug design is most prevalent in oncology, where classical cytotoxic agents can lead to side effects in rapidly dividing cells that are not involved in cancerous tissues or tumor development. Antibody-drug-conjugates (ADCs) offer targeted delivery of potential drugs as selecting a monoclonal antibody (mAb) with a high affinity to a specific antigen in high quantity on the targeted cell's surface, leading to receptor mediated endocytosis for only cells of interest.<sup>3</sup> While cells without high quantities of this antigen are ignored and not exposed to the biologically active drug.

Many of the design features of ADCs have naturally emerged from the medicinal chemistry of prodrugs. Like prodrugs, ADC payloads initially exist in a “chemically masked” form which are biologically impotent until an activation process takes place within the tissue of interest. After ADC internalization from receptor mediated endocytosis, cleavage of the linker occurs in the endolysosome, thereby “unmasking” the payload and allowing for its full biological activity (*Figure 1*). This technology has now led to the approval of ten FDA-approved



ADCs, with approximately 80 ADCs *Figure 1: Mechanism of internalization of an ADC*<sup>24</sup> in over 150 active clinical trial throughout the United States.<sup>4</sup>

The design of an ADC involves optimization of three parts: the antibody, the chemical linkage between the antibody and the payload, and a biologically active payload. The chemical linkage is important for stability of the ADC to prevent untargeted release, while also being responsible for the full release of the payload upon uptake to antigen expressing cell. Fusion of the linker-payload to the antibody is accomplished through conjugation strategies including lysine amide coupling, cysteine coupling, and enzymatic conjugation.<sup>5</sup> Currently, there are several linkage methods specifically designed to be cleaved by lysosomal enzymes such as beta-glucuronidase, legumain, sulfatase, and phosphatase.<sup>6-10</sup> Regardless of the myriad types of ADCs, there are still relatively few methods and linker systems that release payloads containing a hydroxyl functional group, neither by esterase cleavage nor self-immolative spacers. Indeed, the classical “ValCitPABC” linker was based on a protease-cleavable prodrug concept which preceded the advent of modern ADC technology (*Figure 2*).<sup>11-13</sup> However, release from “ValCitPABC” linker can only occur with payloads that contain an amine linkage and cannot occur with hydroxyl containing payloads, despite their wide variety of biological activity.

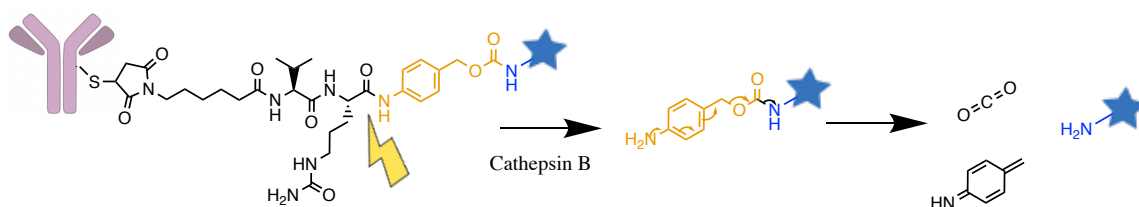


*Figure 2: Release mechanism of payload\* attached to mcValCitPABC linker*

## 1.1 Statement of Purpose

The goal of the studies described herein is to develop a chemical linkage system suitable for ADCs technology that is capable of releasing alcohol containing payloads and evaluating the extent of this release system with other functional groups.

## 2. Simple Esterase Linkage

The most straight forward way to make a linkage system for alcohol containing payloads would be through an ester, attaching the payload to a maleimide which can then be conjugated to an mAb. Throughout this paper, dexamethasone (dex) will be utilized as a glucocorticoid that contains a primary alcohol which can be evaluated for its immune suppression biological activity.

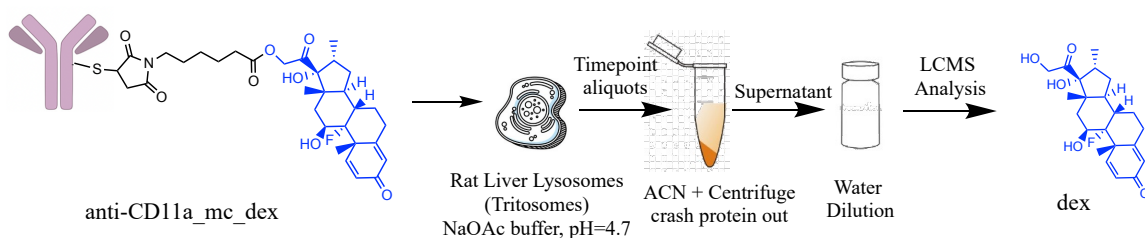


Figure 3: Catabolism of ADCs assay schematic for ester cleavage evaluation

A catabolism assay was conducted with rat liver lysosomes (tritosomes) on the corresponding anti-CD11a\_mc\_dex ADCs to determine if non-specific esterases could cleave the ester bond, resulting in release of dexamethasone. Incubating with tritosomes at a pH of 4.7 (pH of lysosome) simulated the endolysosome catabolism that would follow receptor mediated endocytosis. Aliquots were taken at various time points, protein crashed out, and diluted in water for analysis (Figure 3). Single ion resonance (SIR) analysis indicated detection of only cys\_mc\_dex (biologically inactive), with no detection of dexamethasone as seen in Figure 4 (experiment performed by Courtney Jackson).

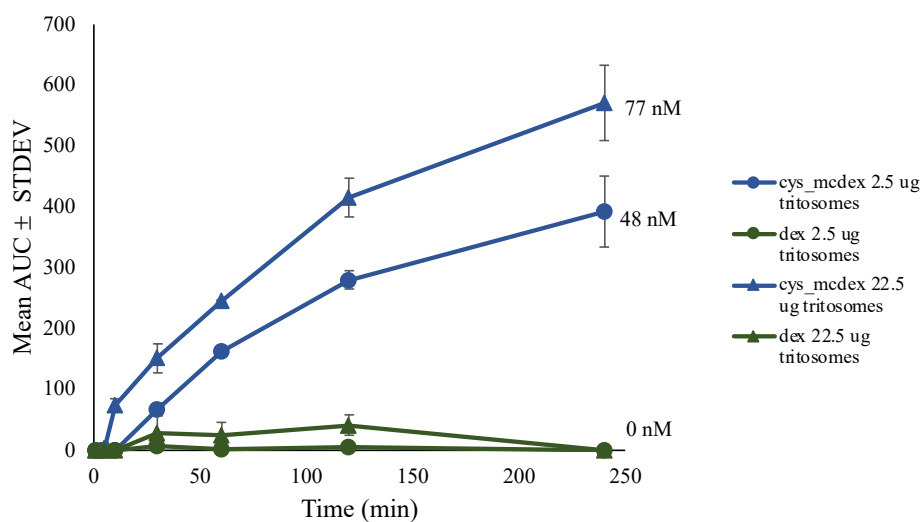
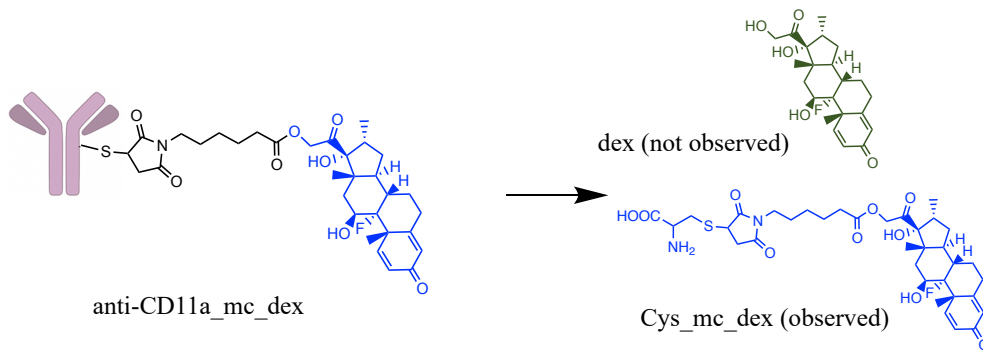
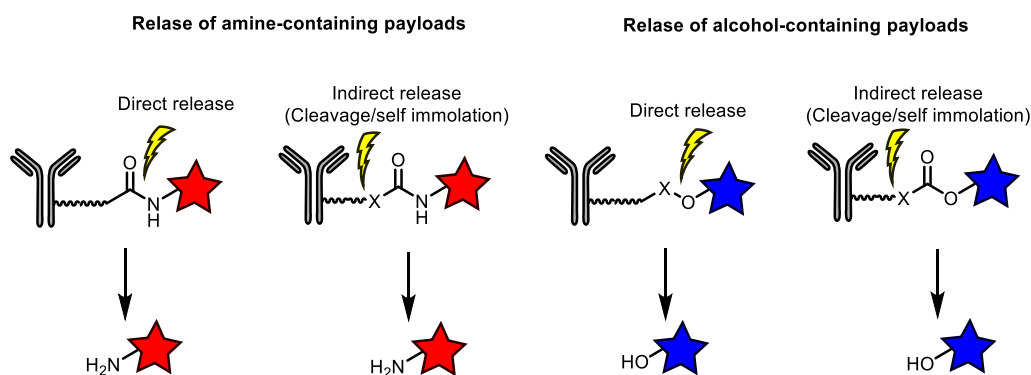


Figure 4: mc\_dex ADC catabolism schematic and catabolism results, need for a self-immolative linker system

Having not seen dexamethasone release from a simple ester linkage to the mAb, a more complex chemical linker must be implemented into the ADC to accomplish release of alcohol containing payloads. To accomplish this, self-immolative linkers can be released from protease cleavable linkers, which then spontaneously release payloads (Figure 5). Modern ADC technology frequently utilizes Cathepsin B cleavage after a ValCit residue leading to the release of a payload attached to a self-immolative spacer. One example of such a self-immolative spacer is the previously mentioned PABC moiety. However, this



spacer is designed to release amine-containing payloads and cannot readily release alcohols. Recent prodrug studies, however, suggest that proline derived spacers, such as a GlyPro residue, may release alcohol payloads by cyclization at neutral pH forming a diketopiperazine (*Figure 6*).<sup>14</sup> Therefore, we hypothesize that a chemical linker containing ValCitGlyPro is well suited to release alcohol containing payloads by lysosomal catabolism cleavage of ValCit, and spontaneous cyclization of GlyPro as seen in *Figure 6*.



*Figure 5: The necessity of a self-immolative linker for alcohol containing payloads*

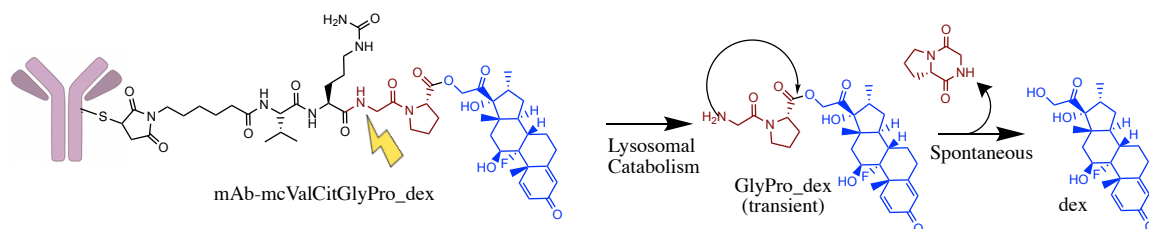


*Figure 6: Novel cleavable linker mechanism for the release of alcohol-containing payloads, such as dexamethasone*

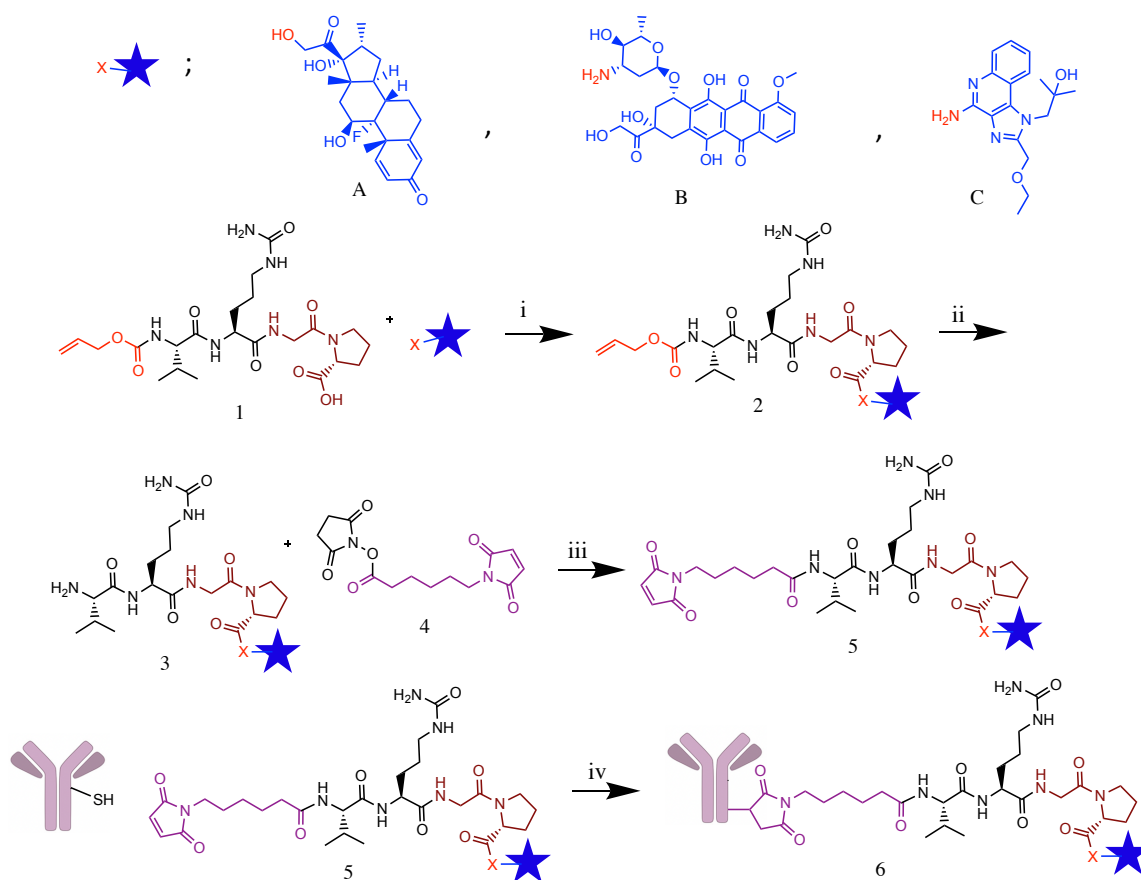
### 3. Synthesis of ValCitGlyPro Linker-payloads and ADCs

The original synthesis was attempted with a one-step coupling between dexamethasone and mpValCitGlyPro-OH. However, the formation of the ester linkage between the two reagents was very challenging considering it needed quite basic conditions, which consequently degraded the maleimide section of the linker, leading to

loss of product. Therefore, a synthesis was formulated that involved a protecting group on the amino terminus so that the sensitive maleimide functional group could be added in the final step.

Synthesis of mcValCitGlyPro linker payloads via a protection of the amino terminus was originally attempted with an fluorenylmethyloxycarbonyl (Fmoc) protecting group of the tetrapeptide (NH<sub>2</sub>\_ValCitGlyPro\_OH). However, after the initial coupling of the carboxy terminus of the peptide and the hydroxyl group on dexamethasone, deprotection resulted in complications within the purification of the linker payload and ultimately loss of product before adding the maleimide to the amino terminus, which is required for antibody conjugation. The synthesis was optimized by replacing the Fmoc protecting group with an alloc protecting group **(1)** (*Figure 7*). The initial coupling of the peptide and payload was conducted using the coupling reagent 1-Ethyl-3-(3-dimethylaminopropyl) carbodiimide (EDC) according to the reaction conditions listed in *Figure 1* and further described in the experimental methods section (*Section 10.2-10.4*). These amino protected linker payloads **(2)** were purified by preparative-HPLC, characterized by UV absorbance and mass spectrometry, and purity was established by UPLC (*Figure S4-S10*). After purification, the alloc group was removed from the linker system, exposing the reactive amino terminus **(3)** which was treated with the activated ester **(4)** to form our final linker payload **(5)** (*Figure 7*). Similar to step i, purification was accomplished by preparative HPLC and evaluated based on UPLC traces. After purification, samples were dried and redissolved in DMA to make a stock solution that was stored in a -80°C freezer **(5)**. Antibodies were reduced using 12eq of TCEP for 2 hours, then buffer exchanged with a 30kDa filtered centrifugal device. 15eq of linker-payload was

added to reduced antibodies for 1.5 hours. Final ADCs (**6**) were purified using a sephadex size-exclusion column (*Figure 7 and Section 10.5*). The concentration of the ADCs was then determined using a Nanodrop (A280) and for aggregation using size exclusion chromatography. The Drug to Antibody Ratio (DAR) was characterized by LCMS, and the mass shift of the modified heavy and light chains (compared to the naked antibody) was measured to confirm the structure (*Figure S1-S3*). Prior to the final synthesis of the ADCs (as demonstrated in *Figure 7*, step iv) the lysosomal payload release of the linker payloads was established as reported below.



- i. alloc\_ValCitGlyPro\_OH (1eq), Payload\* (1.5-3eq), DIEA (1-3eq), HOBt (2-4eq), EDC (2-5eq), DMA, rt, overnight
  - ii. alloc\_ValCitGlyPro\_\* (1eq), Pd (PPh<sub>3</sub>)<sub>4</sub> (.3eq), PhSiH<sub>3</sub> (1.5-3eq), DMA/THF, rt, 1-3 hours
  - iii. NH<sub>2</sub>\_ValCitGlyPro\_\* (1eq), maleimide ester (3-6eq), DMAP (1eq), 2,6 lutidine (4eq), DMA, rt, 2 hours
  - iv. Antibody (1mg), mcValCitGlyPro\_\* (15eq), TCEP (12eq), 5mM EDTA in PBS + 10% DMA, 37°C, 4 hours
- Payloads: dexamethasone (A), doxorubicin (B), resiquimod (C)

*Figure 7: Synthesis of mcValCitGlyPro\_X linker-payloads and ADCs*

Synthesis of mcValCitGlyPro ADCs was also performed with two non-alcohol payloads to understand the role of the leaving group in the self-immolative of the GlyPro dipeptide. Three functional groups were evaluated for GlyPro release: alcohols (A), amines (B), and anilines (C) (Figure 7). All the ADCs were synthesized using the same procedure indicated above and shown in Figure 7. Although the steps and reagents were identical, the only difference was the equivalents used and the yield for each step (see section 10.2-10.4).

#### 4. In Vitro ValCitGlyPro Catabolism Comparison to Non-Cleavable mc Linker

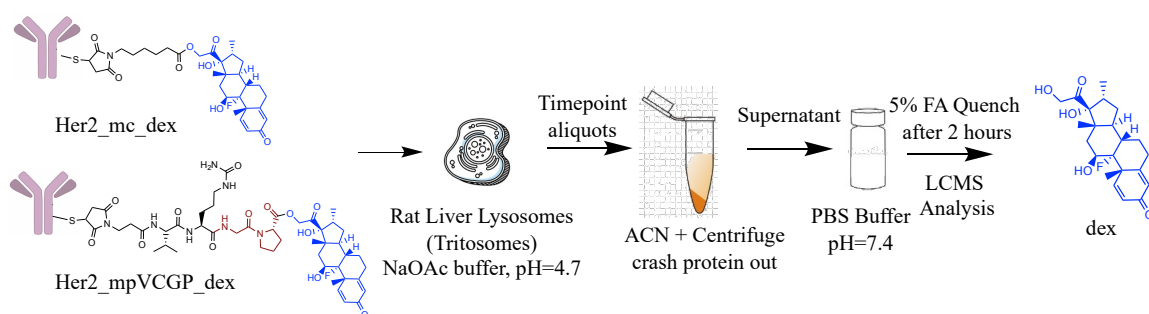
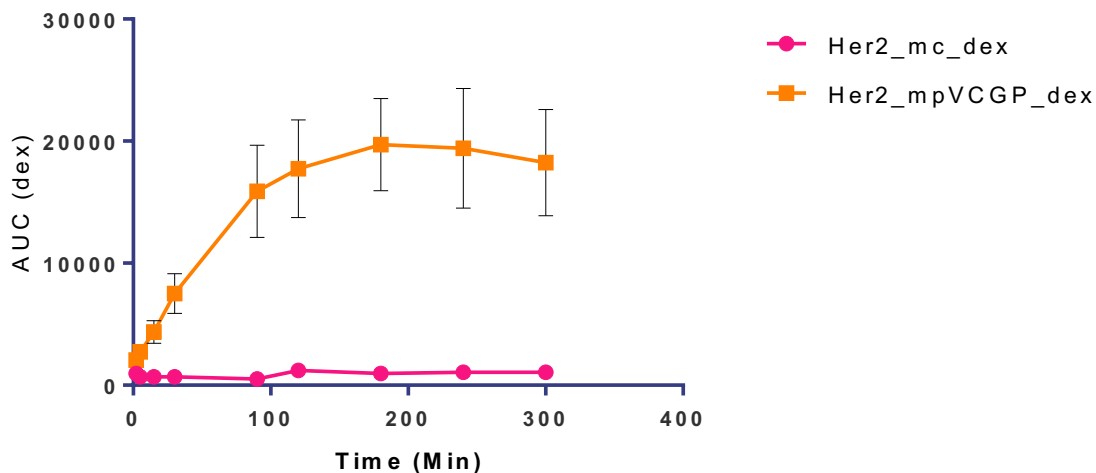


Figure 8: Catabolism schematic of mc\_dex vs mcValCitGlyPro\_dex ADCs

ADCs containing linkers mc\_dex and mpValCitGlyPro\_dex were evaluated in a catabolism assay to determine if the addition of the GlyPro self-immolative spacer increased release of dexamethasone after lysosomal catabolism. A catabolism assay according to Figure 8 was conducted, an additional step including neutralization and quenching of GlyPro cyclization with 5% formic acid in water was added. Results indicated a significant increase in dexamethasone with when the ValCitGlyPro linker was utilized in the ADC in comparison to the non-cleavable mc linker, demonstrating the proposed

mechanism for GlyPro self-immolation is effective in releasing alcohol containing payloads (*Figure 9*).



*Figure 9: ADC containing GlyPro self-immolative linker compared to standard ester linkage for release of dexamethasone*

## 5. Functional group Evaluation for Release from ValCitGlyPro

Based on the pKa of the leaving group resulting from GlyPro cyclization, we hypothesized that GlyPro cyclization will be able to release dexamethasone and not release doxorubicin, with uncertainty around if resiquimod will be release. The alcohol of dexamethasone has a pKa of 15-16, while the amine of doxorubicin has a pKa of ~35. The pKa of conjugated anilines, such as resiquimod, is ~20. This suggests that resiquimod and dexamethasone will be a much better leaving group than the aliphatic amine on doxorubicin.<sup>7</sup> The thermodynamic driving force of the reaction is the formation of a very

stable diketopiperazine, but the kinetics of the reaction are driven by the transition state, and the better the leaving group, the lower the transition state energy.

Based on this hypothesis, mcValCitGlyPro\_X linker payloads (X: dexamethasone, doxorubicin, resiquimod) were evaluated by a catabolism assay meant to simulate the release that would be observed in a cellular assay with ADCs. Linker payloads were first capped with L-cysteine via Michael addition to prevent the reactive maleimide section of the linker payload from reacting with lysosomal proteins which may be cysteine proteases. Following the cysteine capping, linker payloads were incubated with tritosomes for four hours, the protein were crashed out with ACN, the samples diluted with 20xPBS, and then aliquots were quenched with formic acid at various timepoints after cyclization (*Figure 10*). We previously showed that cathepsin B cleavage of the ValCit linker will be complete by ~4h (*Figure 9*) However, the rate of cyclization of the various intermediates was unclear. Thus, the above assay was designed to understand the leaving rate of GlyPro cyclization for the three leaving groups. Note that the 5% formic acid in water was added to halt the cyclization to allow for study of the kinetics of the cyclization. Samples were then evaluated using a Xevo Tandem Quadrupole Mass Spectrometry under the multiple reaction monitoring (MRM), for parent and daughter ions of the payloads released. Scanned transitions for resiquimod are 314.40 → 251.4; transitions for dexamethasone are 373.3 → 147.0, 237.1, and 337.1; transitions for doxorubicin are 545.2 → 332.3, 361.8, and 390.3. All samples were diluted 1:1 with an internal standard of albendazole, with transitions of 265.8 → 192.1 and 234.1. Data was collected, analyzed, and graphed on *Figure 11*.

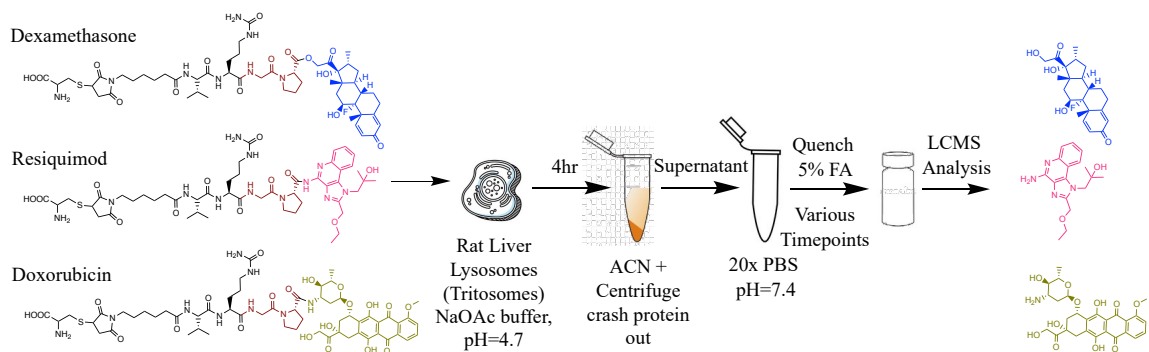


Figure 10: Catabolism assay conditions of *cys\_mcValCitGlyPro\_X* linker-payloads

Results from catabolism assay indicated that only two out of the three linker payloads evaluated resulted in payload release, resiquimod and dexamethasone (Figure 11 and 12). This data indicates that the GlyPro self-immolative spacer has released payloads containing alcohol and aniline linkages, however not amines. The two linker payloads that demonstrated payload release were moved forward into ADCs using the conjugation described in the previous section and in Figure 7, part iv.

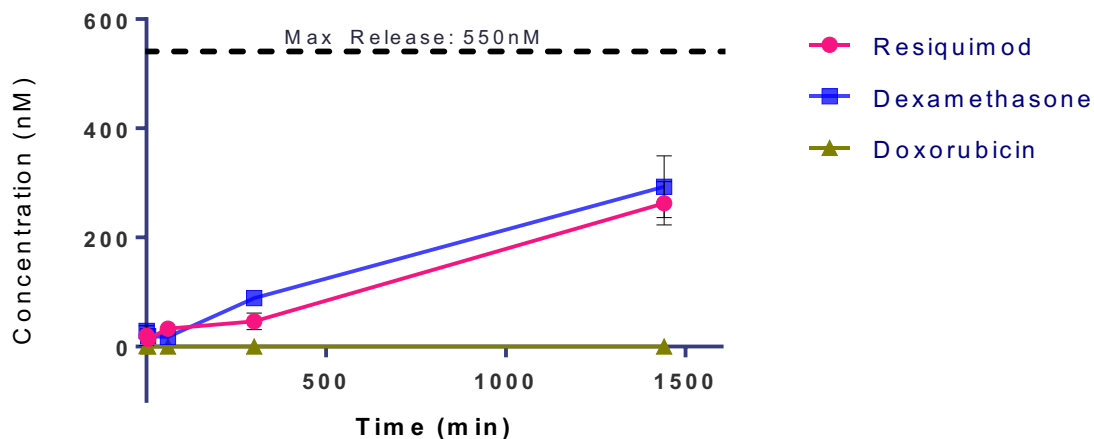


Figure 11: Release of payloads from GlyPro self-immolative linker catabolism

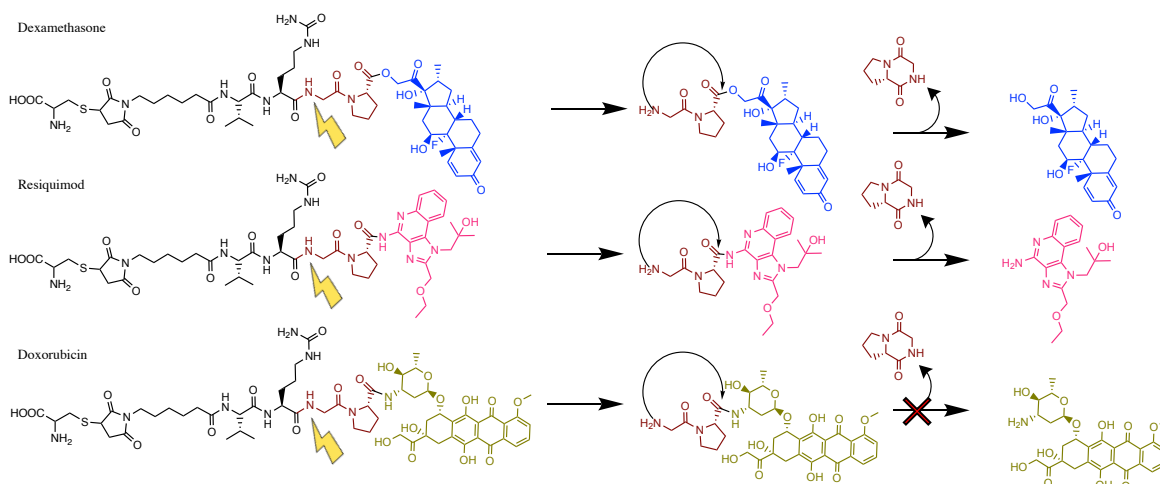


Figure 12: Linker-payload catabolism and cyclization proposed mechanism for payload release

## 6. Immune Activation of Ramos Blue Cells by ValCitGlyPro\_resiquimod ADCs

Resiquimod, being a TLR7/8 agonist, is of high interest for targeted delivery for immuno-activation, for both cancer therapy and as a vaccine adjuvant. TLR7/8 agonists activate the nuclear-factor-kappa-light-chain (NF- $\kappa$ B) to stimulate pro-inflammatory cytokines in lymphocytes.<sup>15</sup> Having detected resiquimod release in vitro, targeted (anti-CD-38) and non-targeted (anti-RSV) ADCs containing mcValCitGlyPro\_resiquimod were evaluated against Ramos Blue Cells, a B lymphocyte cell line that stably expresses an NF- $\kappa$ B/AP-1-inducible secreted embryonic alkaline phosphatase (SEAP) reporter gene. Previous work from our team has shown that CD38 is highly expressed on the surface of Ramos cells and is useful for ADC targeting to this cell type. Targeted and non-targeted ADCs, along with a naked anti-CD-38 mAb, were incubated with Ramos Blue cells at 90ug/mL and 30uL/mL with a cell density of 1.00e6 cells/mL. In addition to the normal growth media (IMDM+10%FBS) 10% human serum was added to block nontargeted antibody uptake. After a four-day incubation period, the supernatant of the targeted ADC



indicated a ~1.7-fold increase of secreted NF- $\kappa$ B, whereas all other samples were at basal levels, in comparison to the control (*Figure 13*). This is consistent with the in vitro data for resiquimod release, while also affirming the targeted release of resiquimod from the ValCitGlyPro linker from ADCs.

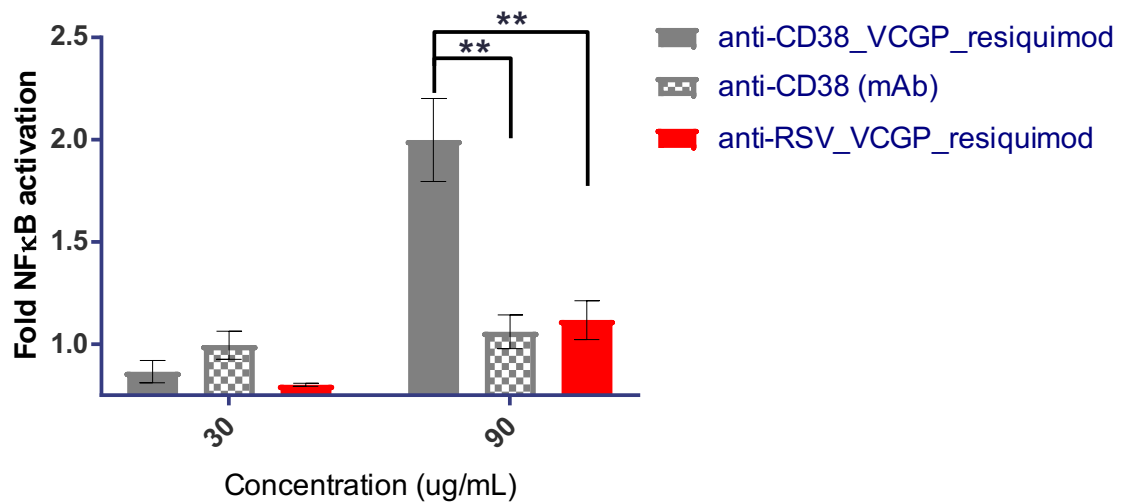


*Figure 13: NF- $\kappa$ B stimulation of Ramos Blue cells from GlyPro containing ADCs.*

## 7. Immune Suppression of Activated Monocytes by ValCitGlyPro<sub>dex</sub> ADCs

In vitro assays were performed to confirm the ability of dexamethasone ADCs to suppress an immune response from human monocytes. Targeted (anti-CD-11a) and non-targeted (anti-Her2) ADCs conjugated to mpValCitGlyPro<sub>dexamethasone</sub> were incubated with THP-1 monocytes. ADCs (or mAb) were evaluated in a dose response assay using a cell density of 2.00e5 cells/mL for 24h, at which time 10ng/mL LPS was added, and incubation was continued for another 24h. The supernatant was evaluated for Tumor Necrosis Factor alpha (TNF $\alpha$ , a pro-inflammatory cytokine) via ELISA. Data demonstrated, as seen in *Figure 14*, that the targeted ADC was approximately 10-fold more

potent at preventing cell stimulation by LPS than the untargeted ADC, both significantly different from naked antibodies (experiment conducted by Siteng Fang).

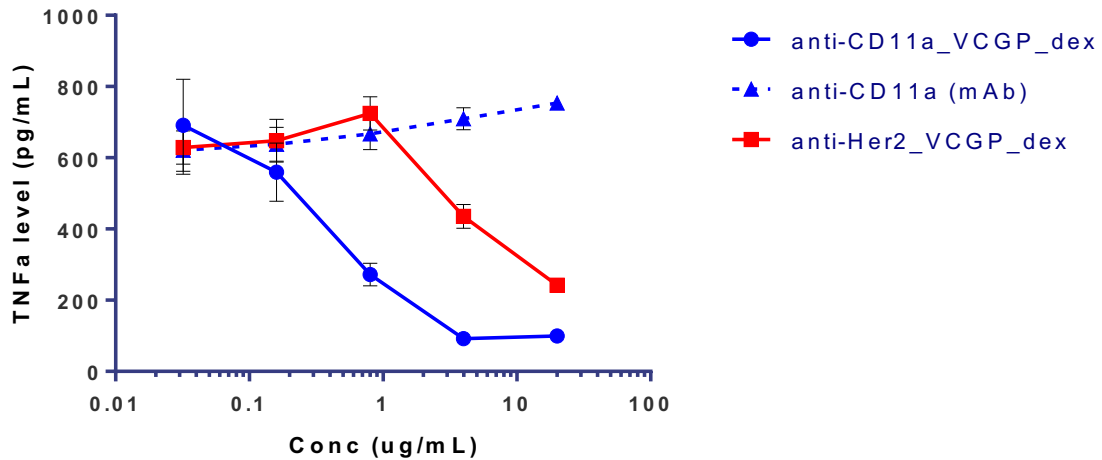


Figure 14: TNF $\alpha$  suppression after LPS stimulation by targeted and untargeted dexamethasone ADCs

To follow up on these results, an experiment was designed to evaluate the activation of pro-inflammatory transcription factors in THP-1 monocytes, with the goal of identifying the most effective cell-surface antigen target for ADC delivery. To accomplish this, an ADC suppression screen with a dual reporter monocyte cell line (THP-1 dual, Invivogen). THP-1 dual monocytes contain both a NF- $\kappa$ B reporter (SEAP) and an interferon regulatory factors (IRF) reporter (secreted luciferase, Lucia). Initially, a screen was used on all ADCs and mAb at 30ug/mL and 6ug/mL. Cells were incubated at a 2.00e5 cells/mL density with ADCs for 4 hours at which time they were stimulated with 1ng/mL LPS for another 16 hours. Supernatant was then tested for SEAP and Lucia. We anticipated that ADCs of interest would block the NF- $\kappa$ B or IRF signaling pathways while the naked mAb and the control (nontargeted) ADC would not. The incubation was conducted in the presence of 10% human serum (v/v) to decrease the amount of non-targeted uptake of ADCs. Results

indicated that anti-TNF $\alpha$  ADCs significantly decreased NF- $\kappa$ B production in comparison to the positive control (LPS alone), the non-targeted ADC (anti-RSV), and the naked anti-TNF $\alpha$  mAb (*Figure 15*). A decrease in the IRF pathway was also observed for anti-TNF $\alpha$  ADCs, however due to low stimulation of the IRF pathway, results are inconclusive and a notable suppression from non-targeted ADCs (*Figure 15*). Although other ADCs indicated a suppression, TNF $\alpha$  ADCs were most promising and evaluated at a lower concentration. Interestingly and unexpectedly, the anti-CD11a ADC exhibited only weak activity in this assay, in contrast to the functional assay shown in *Figure 14*.

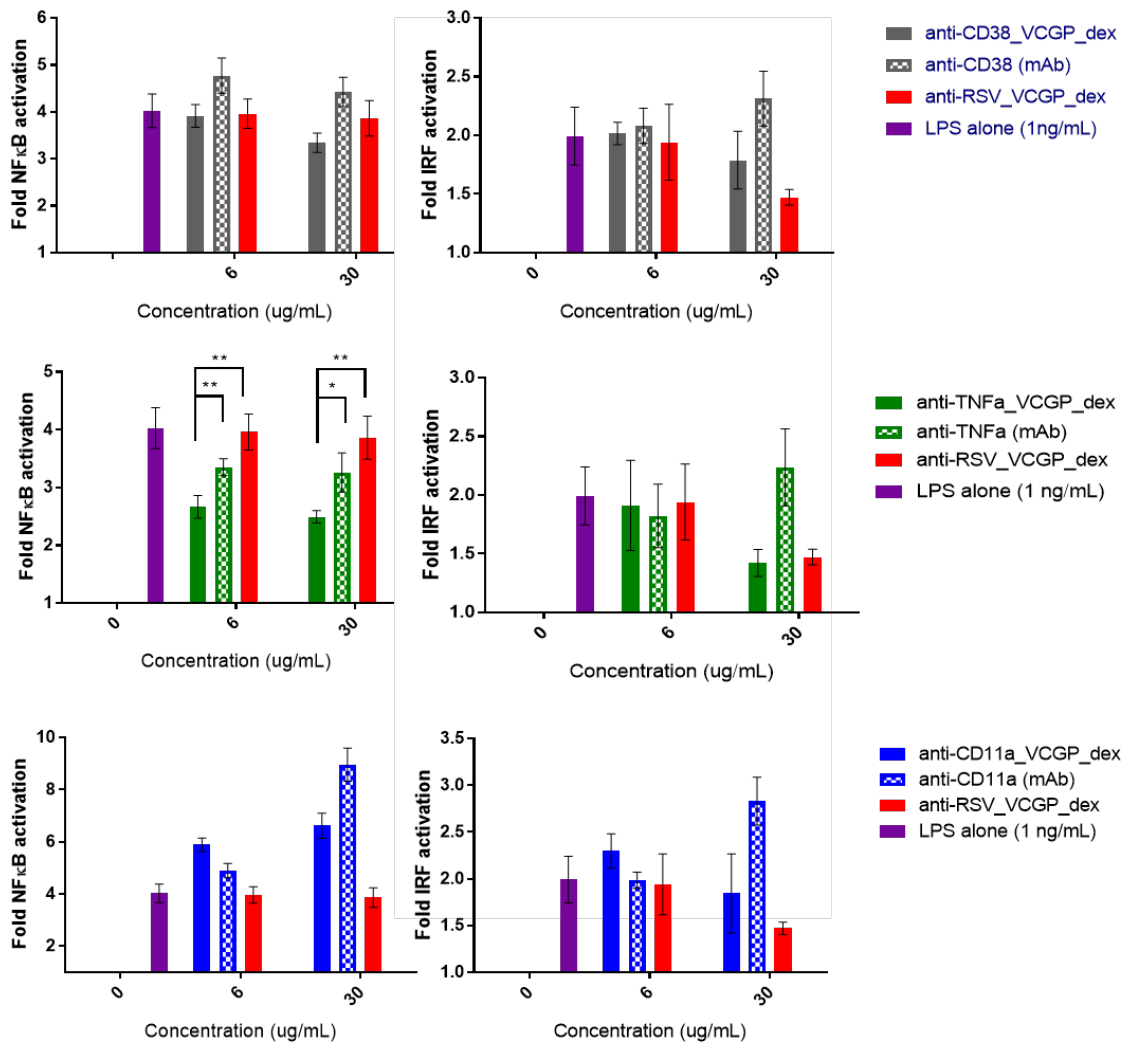
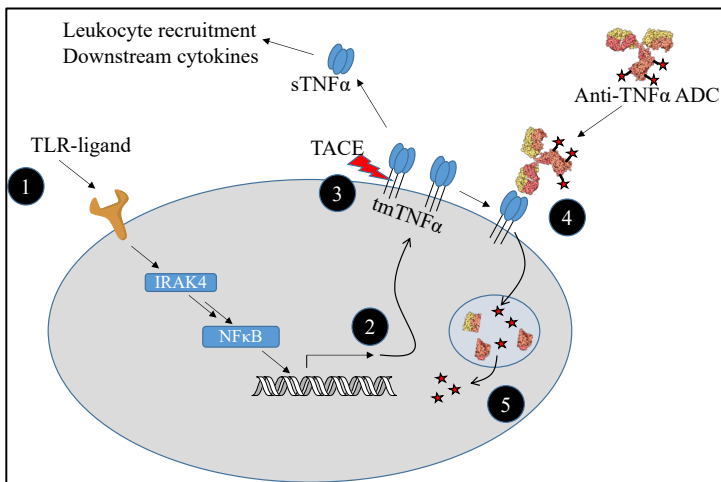


Figure 15: mpValCitGlyPro\_dex ADC screen for THP-1 suppression assay, NF- $\kappa$ B (left) and IRF (right) decrease after 1ng/mL LPS stimulation

## 8. Dose Response of anti-TNF $\alpha$ ADCs containing mpValCitGlyPro\_dex

TNF $\alpha$  is most one of the most prevalent cytokines for several inflammatory diseases, such as rheumatoid arthritis (RA). Anti-TNF $\alpha$  mAb therapy is a clinically successful way to decrease inflammation by decreasing plasma levels of TNF $\alpha$  and therefore, downstream cytokines, such as IL-1, IL-6, and IL-8.<sup>16,17</sup> However, a significant portion of patients are resistant to this therapy type, which increases the necessity for improved therapeutics. Naturally, adding a potent glucocorticoid such as dexamethasone through ADC technology would allow an improved immune suppression to the anti-TNF $\alpha$  mAbs. TNF $\alpha$  production begins with the expression of a transmembrane TNF $\alpha$  (tmTNF $\alpha$ ) that is converted into secreted TNF $\alpha$  (sTNF $\alpha$ ) by TNF $\alpha$  converting enzyme (TACE).



Therefore, adding an inhibitor to this enzyme may perhaps increase tmTNF $\alpha$  and therefore increase receptor mediated endocytosis of anti-TNF $\alpha$  ADCs (Figure 16).

Figure 16: Schematic illustration of tmTNF $\alpha$  and TACE

With this in mind, we performed an experiment to better understand the role of TACE in the uptake of TNF $\alpha$  ADCs. As seen in Figure 16, stimulation of THP-1 monocytes with 1ng/mL LPS increases the production of NF- $\kappa$ B production ~8-10 fold.

The addition of the anti-TNF $\alpha$  ADC containing ValCitGlyPro\_dex results in a dose-dependent reduction in NF- $\kappa$ B signaling. However, the naked anti-TNF $\alpha$  mAb was able to suppress the signaling of NF- $\kappa$ B as well, but not as significantly as the ADC. An ADC with the same ValCitGlyPro\_dex linker payloads with an untargeted isotype mAb (anti-RSV), did not cause any significant decrease in NF- $\kappa$ B in comparison to the naked anti-TNF $\alpha$  mAb and the anti-TNF $\alpha$  ADC. Therefore, both the targeted mAb and the conjugation with the appropriate linker-payload system is necessary for increasing monocyte suppression. Importantly, addition of the TACE inhibitor did seem to increase the immunosuppressive activity of the ADC as hypothesized above (*Figure 17*, bottom panel). Unfortunately, the IRF pathway did not have a large enough stimulation window to allow us to make any significant claims about the suppression.

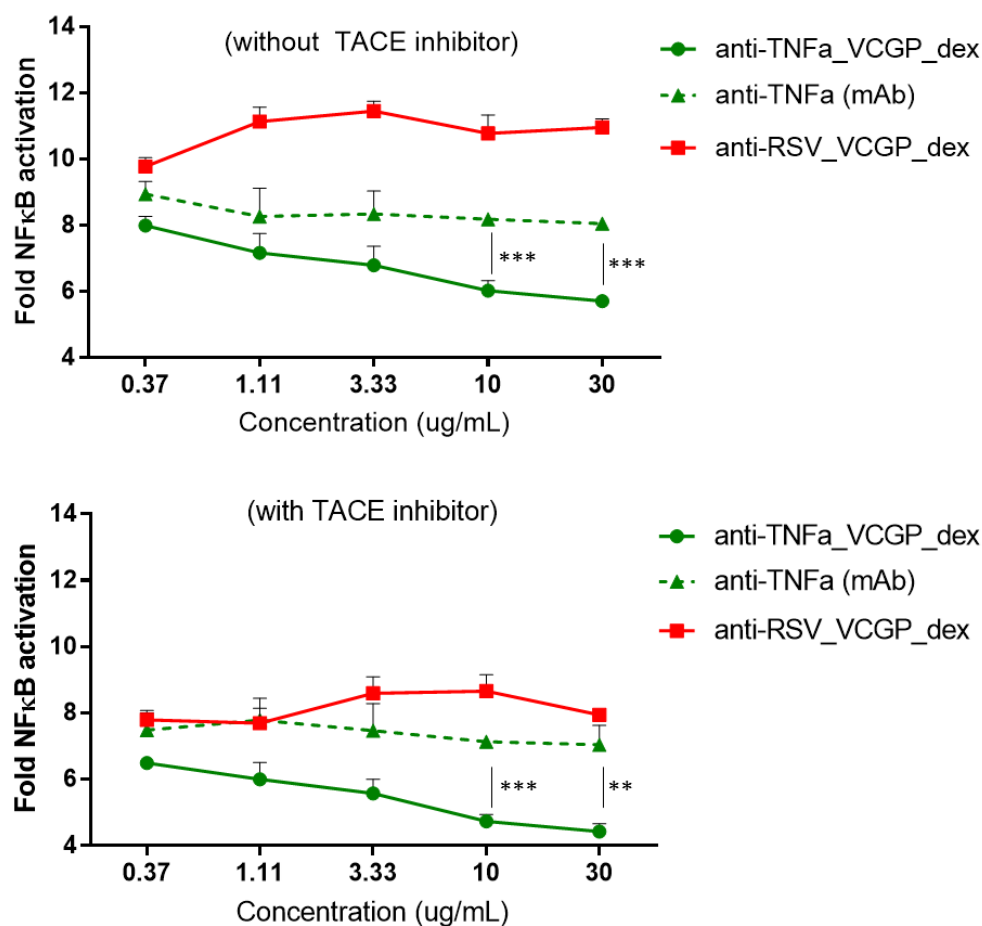


Figure 17: THP-1 monocyte NF- $\kappa$ B suppression after 1ng/mL LPS stimulation, dose response of ValCitGlyPro<sub>dex</sub> ADCs with and without TACE inhibitor

## 9. Discussion and Conclusions

We report, to the best of our knowledge, one of the first systematic study of evaluating the suitability of simple esters as cleavable linkers for the release of alcohols. Numerous groups have reported various strategies for the release of alcohol-containing payloads from ADCs, including the use of phosphatase-cleavable linkers, methylene-alkoxy self-immolative spacers, and self-immolative carbamate spacers.<sup>9,18,19</sup> In spite of

the implementation of ester-containing linkers have been used in ADC design<sup>10</sup>, there have been no reports evaluating their cleavage upon uptake into antigen-expressing cells. Results from ADCs containing a simple ester linkage between dexamethasone and a maleimidocaproyl (mc), determined that upon lysosomal cleavage, complete ADC catabolism resulted in formation of a cyc-mc\_dex product with no detection of dex by itself during the time course of the experiment (*Figure 4*). This observation is an indication that to reach desired concentrations of dexamethasone from ADCs, a fast self-immolative spacer is imperative to by-pass the lack of esterase cleavage.<sup>20</sup> By employing the classically used, Cathepsin B cleavable, ValCit linker, the addition of a GlyPro dipeptide was evaluated for the steric benefit, rapid cyclization rate of five-membered rings, and prodrug success of proline containing payloads.<sup>14,21</sup> After successful synthesis of several linker-payloads containing ValCitGlyPro, this hypothesis was confirmed to hold true, as rapid cyclization of GlyPro resulted in release of dexamethasone and resiquimod, expanding to anilines as well as alcohol-containing payloads (*Figure 9 and 11*).

Not only was release detected after ADC catabolism, but several cellular assays concluded the desired biological activity of payloads released from ADCs. Targeted delivery of a TLR 7/8 agonist, resiquimod, was accomplished in B-cells (*Figure 13*). This may be an effective way to activate B-cells for a possible vaccine adjuvant (allowing less vaccine and less side effects during immunizations) along with activating tumor associated macrophages to enhance phagocytosis of cancer cells.<sup>22,23</sup> Conversely, dexamethasone was demonstrated to release from ValCitGlyPro ADCs at a concentration high enough to suppress the NF- $\kappa$ B and TNF $\alpha$  (pro-inflammatory transcription factor and cytokine, respectively) from monocytes stimulated by LPS (*Figure 15*). The suppression of

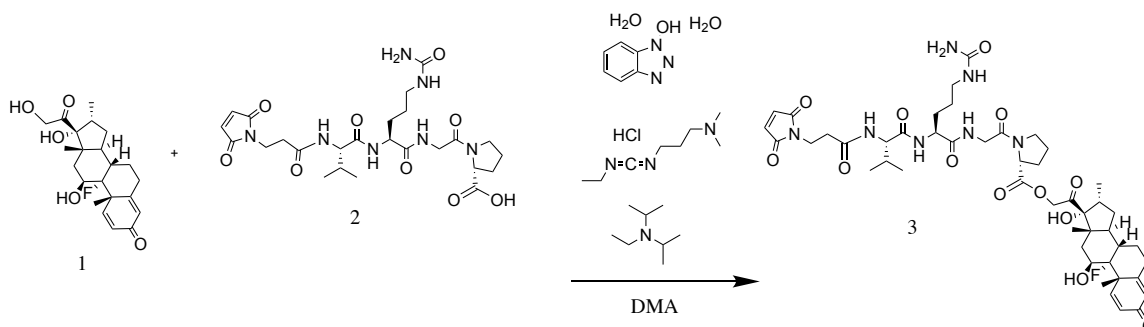
monocytes was further enhanced by conjugation to anti-TNF $\alpha$  mAb (*Figure 15 and 17*), which are already a commonly treatment for rheumatoid arthritis and a potential treatment against a wide array of autoimmune diseases.<sup>16,17</sup> Conjugation with dexamethasone decreased this immune response and with the longevity of mAb, could perhaps increase the length of time that patients decrease their immune system inflammation. Adding a TACE (TNF $\alpha$  converting enzyme) inhibitor was also demonstrated to increase internalization of ADCs, therefore increased ADC catabolism and dexamethasone released. We conclude that the addition of the GlyPro dipeptide into the well-studied ValCit linker system has allowed for the design of ADC technology to release alcohol containing payloads while also having the capacity to release aniline containing payloads.

Future work in this project involves conducting proton NMRs of the three linker-payloads containing ValCitGlyPro, to confirm the linkage described above. Additionally, human and mouse plasma studies of the ADCs containing ValCitGlyPro linkers will be performed. Stability of this linkage system in human and mouse plasma would assist in determination if such a linkage is suitable for in vivo studies and to determine if non-targeted release could occur during the longevity of antibody proteins in the human body. Finally, ValCitGlyPro\_dexamethasone ADCs will also be evaluated for immune suppression in a similar way as above, however, quantifying several inflammatory cytokines in the supernatant.



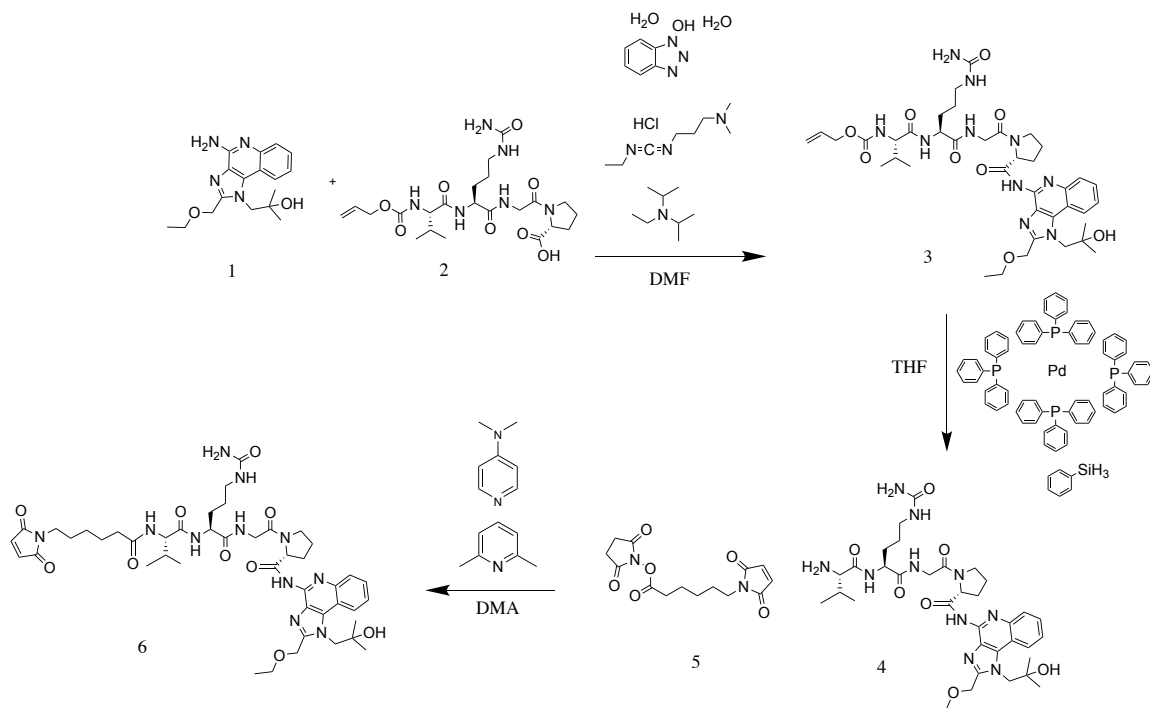
## 10. Experimental Methods

### 10.1 Organic Synthesis of mpValCitGlyPro\_dexamethasone



mpValCitGlyPro\_OH (**2**) (10.8mg, 1.1eq, 18.6umol), 1-Ethyl-3-(3-dimethylaminopropyl) carbodiimide (EDC) (13.0mg, 4.0eq, 67.8umol), 1-Hydroxybenzotriazole (HOBt) (2.6mg, 1eq, 16.9umol), and N,N-Diisopropylethylamine (DIEA) (6.57mg, 8.9uL, 3eq, 50.8umol) was combined in 500uL Dimethylacetamide (DMA) at a reaction molarity of 40mM, stirred for 30 minutes at room temperature before adding dexamethasone (**1**) (6.7mg, 1.0eq, 16.9umol). Yield seemed low after 14 hours therefore mpValCitGlyPro\_OH (**2**) 10.8mg, 1.1eq, 18.6umol), EDC (13.0mg, 4.0eq, 67.8umol), and DIEA (6.57mg, 8.9uL, 3eq, 50.8umol) were added to solution and stirred for another 2.5 hours. The resulting mpValCitGlyPro\_dexamethasone (**3**) was purified through normal preparative HPLC and concentrated to dryness, for a yield of 5.8mg (16.9umol, 36%). LCMS (normal analytical HPLC method): (M+H)<sup>+</sup> 554.6 Da, Retention time: 2.69 min (Figure S4). The final linker-payload was dissolved in DMA to make a 5mM stock solution and stored at -80°C (this experiment was conducted by Kelsey Watts).

## 10.2 Organic Synthesis of mcValCitGlyPro\_resiquimod

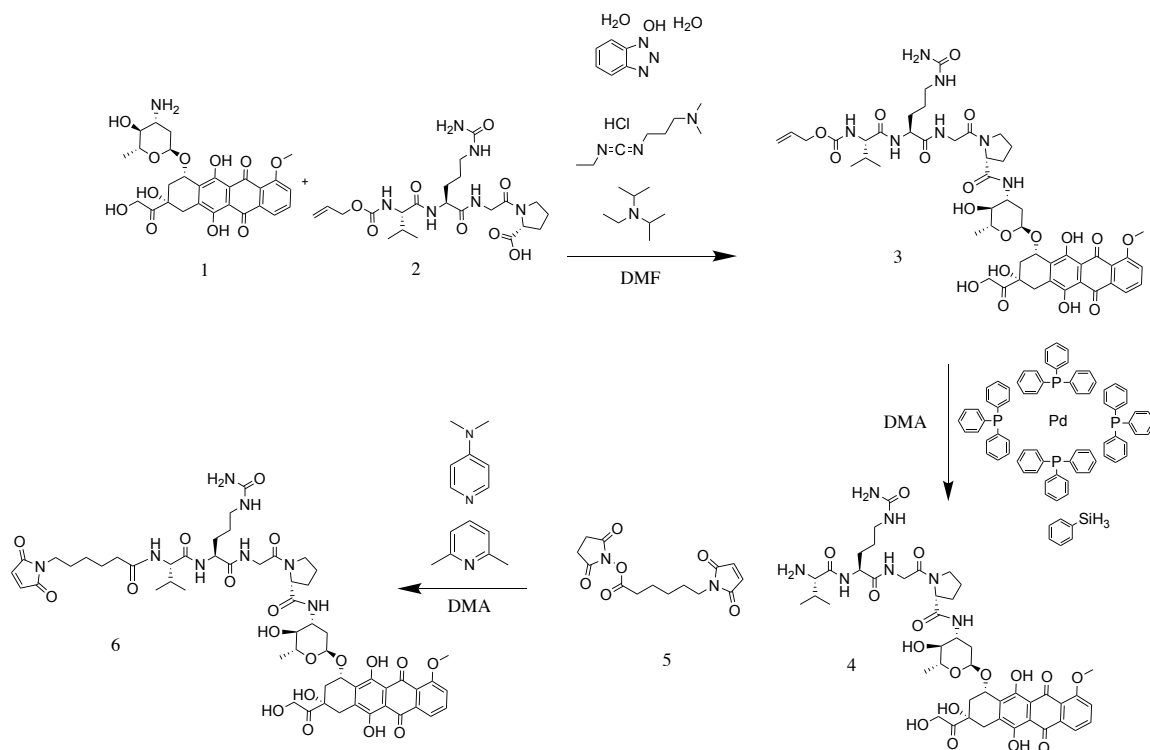


Resiquimod (**1**) (4.6mg, 1.5eq, 15umol), alloc\_ValCitGlyPro\_OH (**2**) (5.0mg, 1.0eq, 9.8umol), EDC (7.5mg, 4.0eq, 39umol), HOBt (3.3mg, 2eq, 20umol), and DIEA (1.3mg, 1.7uL, 1eq, 9.8umol) was combined in 300uL anhydrous N,N-Dimethylmethanamide (DMF) at a reaction molarity of 32mM, stirred for 48 hours at room temperature. The resulting alloc\_ValCitGlyPro\_resiquimod (**3**) was purified through normal preparative HPLC and concentrated to dryness, for a yield of 4.0mg (4.9umol, 51%). LCMS (normal analytical UPLC method): (M+H)<sup>+</sup> 809.6 Da, Retention time: 2.38 min (*Figure S5*).

Alloc\_ValCitGlyPro\_resiquimod (**3**) (4.0mg, 4.9umol) was redissolved in 600uL of Tetrahydrofuran (THF) and 200uL (2.0mg, 2.5umol,) was moved forward to deprotection. Phenylsilane (1.1mg, 4eq, 9.9umol) and Tetrakis(triphenylphosphine)palladium (0.89mg, 0.3eq, 0.74umol) were added to the

300uL THF solution for a final reaction molarity of 8.2mM, this was left at room temperature for 30 minutes before full deprotection (**4**), confirmed by LCMS. Solution was concentrated to dryness and redissolved in 300uL of DMA. 6-Maleimidohexanoic acid N-hydroxysuccinimide ester (**5**) (2.8mg, 3.6eq, 2.5umol), 2,6-Lutidine (1.1mg, 1.2uL, 4.0eq, 9.9umol), and DMAP (0.30mg, 1.0eq, 2.5umol) were added to the 300uL DMA solution for a final reaction molarity of 8.2mM. Reaction was let stir for 1.5 hours before adding more maleimide (**5**) (1.5mg, 2.0eq, 2.5umol) and 2,6-Lutidine (0.55mg, 0.6uL, 2.0eq, 9.9umol). Reaction was left stirring for 24 hours at room temperature and was purified through normal preparative HPLC. LCMS (normal analytical UPLC method): (M+H)<sup>+</sup> 918.6 Da, Retention time: 2.38 min (Figure S6). Fractions were concentrated to dryness and 0.60mg of mcValCitGlyPro\_resiquimod (**6**) were collected (0.7umol, 30% yield for last two reactions). The final linker-payload was dissolved in DMA to make a 5mM stock solution and stored at -80°C.

### 10.3 Organic Synthesis of mcValCitGlyPro\_doxorubicin

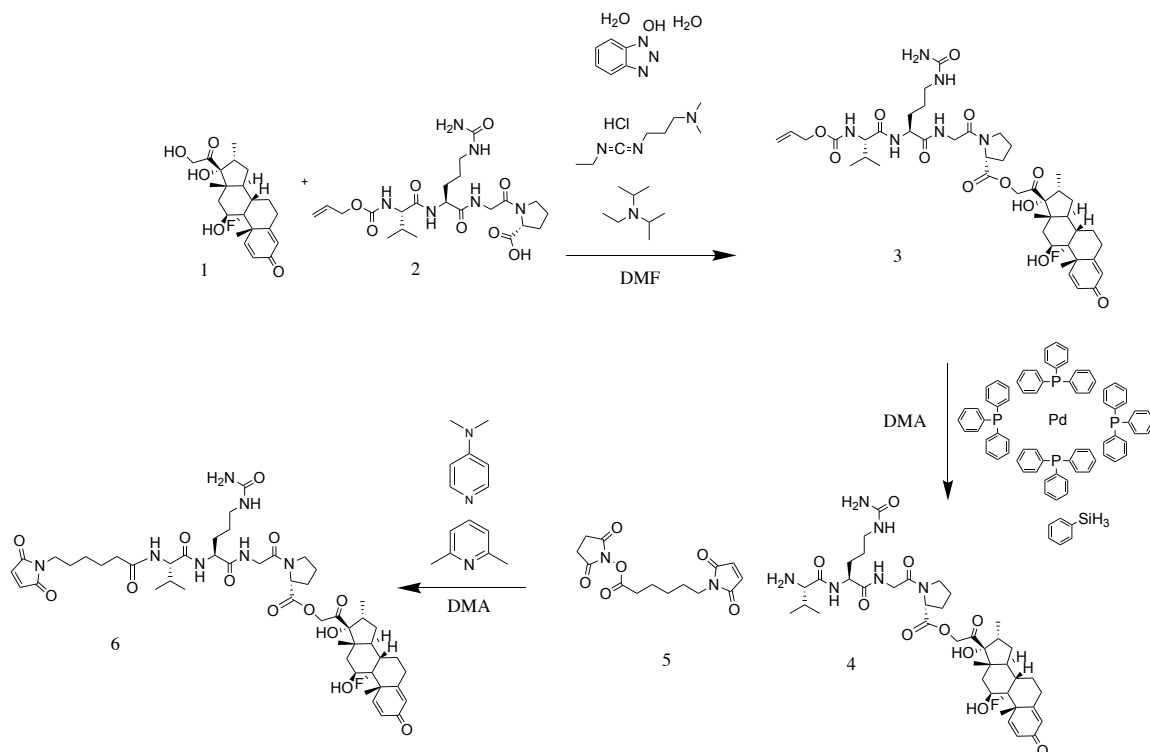


Doxorubicin (**1**) (8.5mg, 1.5eq, 15umol), alloc\_ValCitGlyPro-OH (**2**) (5.0mg, 1.0eq, 9.8umol), EDC (3.7mg, 2.0eq, 20umol), HOBt (3.3mg, 2eq, 20umol), and DIEA (1.3mg, 1.7uL, 1eq, 9.8umol) was combined in 300uL anhydrous DMF at a reaction molarity of 32mM, stirred for 5 hours at room temperature. The resulting alloc\_ValCitGlyPro\_doxorubicin (**3**) was purified through normal preparative HPLC and concentrated to dryness, for a yield of 5.8mg (9.8umol, 57%). LCMS (normal analytical UPLC method): (M+Na)<sup>+</sup> 1060.5 Da, Retention time: 2.78 min (*Figure S7*).

Alloc\_ValCitGlyPro\_doxorubicin (**3**) (5.8mg, 9.8umol) was redissolved in 500uL DMA was moved forward to deprotection. Phenylsilane (2.4mg, 4eq, 22umol) and Tetrakis(triphenylphosphine)palladium (1.9mg, 0.3eq, 1.7umol) were added to the 500uL DMA solution for a final reaction molarity of 11mM, this was left at room temperature for 5 minutes before full deprotection (**4**), confirmed by LCMS. Air was blown over reaction

solution till the volume was 400uL. 6-Maleimidohexanoic acid N-hydroxysuccinimide ester (**5**) (6.2mg, 3.6eq, 20umol), 2,6-Lutidine (2.4mg, 2.6uL, 4.0eq, 22umol), and DMAP (0.68mg, 1.0eq, 5.6umol) were added to the 400uL DMA solution for a final reaction molarity of 14mM. Reaction was left stirring for 1 hours at room temperature and was purified through normal preparative HPLC. Along with the desired linker-payload, there was a +2 peak, indicating the reduction of the maleimide double bond, however this would not interfere with antibody conjugation. Fractions were concentrated to dryness and 1.5mg of mcValCitGlyPro\_doxorubicin (**6**) were collected (1.3umol, 24% yield for last two reactions). LCMS (normal analytical UPLC method): (M+Na)<sup>+</sup> 1069.7 Da, Retention time: 2.73 min (*Figure S8*). Considering the impurity is most likely the reduction of the maleimide double bond, the catabolism study following this synthesis was still conducted as this should not interfere with cleavage after ValCit. The final linker-payload was dissolved in DMA to make a 5mM stock solution and stored at -80°C.

## 10.4 Organic Synthesis of mcValCitGlyPro\_dexamethasone



Dexamethasone (**1**) (5.7mg, 1.5eq, 14.6umol), alloc\_ValCitGlyPro\_OH (**2**) (10.0mg, 2.0eq, 19.5umol), EDC (5.6mg, 3.0eq, 29.3umol), HOBt (3.3mg, 2eq, 19.5umol), and DIEA (1.3mg, 1.7uL, 1eq, 9.8umol) was combined in 300uL anhydrous DMF at a reaction molarity of 64.7mM, stirred for 24 hours at room temperature. Yield seemed low therefore alloc\_ValCitGlyPro\_OH (**2**) (5mg, 1eq, 8.8umol), EDC (3.7mg, 2.0eq, 19.3umol), HOBt (3.3mg, 2eq, 19.5umol), and DIEA (2.6mg, 3.4uL, 2eq, 19.6umol) were added to solution and stirred for another 24 hours. The resulting alloc\_ValCitGlyPro\_dexamethasone (**3**) was purified through normal preparative HPLC and concentrated to dryness, for a yield of 2.1mg (9.8umol, 24%). LCMS (normal analytical UPLC method): (M+H)<sup>+</sup> 887.6 Da, Retention time: 3.08 min (*Figure S9*).

Alloc\_ValCitGlyPro\_dexamethasone (**3**) (2.1mg, 9.8umol) was redissolved in 500uL DMA was moved forward to deprotection. Phenylsilane (0.38mg, 1.5eq, 3.6umol)

and Tetrakis(triphenylphosphine)palladium (0.82mg, 0.3eq, 0.71umol) were added to the 500uL DMA solution for a final reaction molarity of 4.7mM, this was left at room temperature for 10 minutes before full deprotection (**4**), confirmed by LCMS. Air was blown over reaction solution till the volume was 400uL. 6-Maleimidohexanoic acid N-hydroxysuccinimide ester (**5**) (2.2mg, 3.0eq, 7.1umol), 2,6-Lutidine (1.0mg, 1.1uL, 4.0eq, 9.5umol), and DMAP (0.29mg, 1.0eq, 2.4umol) were added to the 400uL DMA solution for a final reaction molarity of 5.9mM. Reaction was left stirring for 2 hours at room temperature and was purified through normal preparative HPLC. Fractions were concentrated to dryness and 2.2mg of mcValCitGlyPro\_dexamethasone (**6**) were collected (2.2 umol, 93% yield for last two reactions). LCMS (normal analytical UPLC method): (M+H)<sup>+</sup> 996.7 Da, Retention time: 3.04 min (*Figure S10*). The final linker-payload was dissolved in DMA to make a 5mM stock solution and stored at -80°C

### 10.5 mAb Conjugation Procedure

mAb (1mg) was treated with 12 equivalents of 5mM tris(2-carboxyethyl) phosphine (TCEP) and 0.1 M phosphate buffered saline (PBS) pH 7.4 with 5 mM Ethylenediamine tetraacetic acid (EDTA) was added to the reaction to have a final volume of 500uL (2.0mg/mL concentration of mAb). Solution was heated at 37°C for two hours. The reaction was buffer exchanged and concentrated using a centrifuge spin device with a 30KDa filter. Linker-payload (15eq) in DMA were added to the reduced mAb along with 0.1 M PBS pH 7.4 with 5 mM EDTA and DMA to make the final volume 5-10% organic. Reaction sat at room temperature for 1.5 hours, then buffer exchanged using a Sephadex column according to the manufacture's protocol. An aliquot was reduced using TCEP and tested for its loading using HPLC-MS and the drug to antibody ratio (DAR) was calculated.

The concentration of ADC was calculated using a Nanodrop using the Protein A290 IgG method and aggregation of an unreduced aliquot was analyzed using size-exclusion chromatography on a UPLC or NGC Chromatography System Bio-Rad. ADCs were sterilized, logged, and stored at 4°C.

### **10.6 Lysosomal Catabolism, mc\_dex ADCs**

13ug of ADCs were independently buffer exchanged from PBS to NaOAc buffer (pH=4.7) and concentrated to 30uL using a centrifuge spin column, for a final concentration of 0.43mg/mL. Separately, 2.00uL of 1M Dithiothreitol (DTT) was diluted into 998uL NaOAc buffer for a 2mM DTT solution. Rat Liver Lysosomes (tritosomes) (1uL, 2.5mg/mL, 2.5ug) was added to 11uL of 2mM DTT and 8uL NaOAc buffer. This mixture was incubated at 37°C for 15 minutes. 20uL of activated tritosomes (2.5ug) was added to the 30uL of the ADCs and incubated at 37°C. 5uL aliquots were taken at 1, 5, 15, 30, 60, 120, and 240 minutes, to which 45uL Acetonitrile (ACN) was added to crash out proteins, samples were immediately vortexed and centrifuged at max speed for 5 minutes. 40uL was carefully taken from the top and added to 80uL of water. For analysis, 20uL was injected into a UPLC using the single ion resonance (SIR) method for 393.24 m/z and compared to a standard curve that was generated (experiment conducted by Courtney Jackson).

### **10.7 lysosomal Catabolism, mc\_dex vs mpValCitGlyPro\_dex ADCs**

30ug of ADCs were independently buffer exchanged from PBS to NaOAc buffer (pH=4.7) and concentrated to 60uL using a centrifuge spin column, for a final concentration of 0.5mg/mL for each ADC. Separately, 2.00uL of 1M DTT was diluted into 998uL NaOAc buffer for a 2mM DTT solution. Tritosomes (7uL, 2.5mg/mL, 17.5ug) was



added to 77uL of 2mM DTT and 56uL NaOAc buffer. This mixture was incubated at 37°C for 15 minutes. 40uL of activated tritosomes (5.0ug) was added to the 60uL of each ADC separately and incubated at 37°C. 10uL aliquots were taken at 1, 5, 10, 15, 30, 60, 120, 180, and 240 minutes, to which 90uL ACN was added to crash out proteins, samples were immediately vortexed and stored at -80°C till all samples were collected.

All samples were thawed before centrifuged for 5 minutes. 80uL was carefully removed from the supernatant of each sample and transferred into a LCMS vial with 80uL of PBS (pH=7.4). All samples were incubated at 37°C for 2 hours to allow for cyclization of the GlyPro spacer for release of dex. After 2 hours, 10uL of 5% formic acid in water was added to each vial to halt cyclization. 10uL injections were analyzed on a UPLC using the single ion resonance (SIR) method for 393.24 m/z and compared to a standard curve that was generated (experiment conducted and designed by Kelsey Watts, analysis by Justin Howe).

### **10.8 Lysosomal Catabolism, Linker-payload Leaving Group Ability from GlyPro**

All linker-payloads were initially diluted down to 1mM in a DMA solution and a 5mM stock of L-cysteine in PBS was made. mcValCitGlyPro\_X (20ug, 20uL, 1.0mM, 1eq, 0.020umol) and L-cysteine (12ug, 20uL, 5.0mM, 5eq, 0.10umol) were mixed in an Eppendorf tube and a small aliquot was ran after 15 minutes on a UPLC to confirm Michael addition. 10uL of Cys\_mcValCitGlyPro\_X was added to 90uL of NaOAc buffer (pH=4.7) (final concentration of 50uM). Separately, 2.00uL of 1M DTT was diluted into 248uL NaOAc buffer for a final concentration of 8mM DTT. Rat Liver Lysosomes (tritosomes) (18uL, 2.5mg/mL, 45ug) was added to 50uL of 8mM DTT and 25uL NaOAc buffer. This mixture was incubated at 37°C for 15 minutes. 30uL of activated tritosomes was then mixed

with 30uL of 50uM cysteine capped linker-payload and incubated at 37°C. After 30 minutes and 4 hours, 30uL aliquots were removed and 60uL of ACN to crash out proteins, solution was immediately vortexed and centrifuged at 10,000rpm for 10 minutes. 75uL of supernatant was removed at this point and stored at -80°C till the second half of the assay.

Samples were thawed and 75uL of 20x PBS to neutralize the solution, simulating leaving the lysosome. Samples incubated at 37°C to allow for GlyPro cyclization, 30uL aliquots were removed at 0, 5, 60, 300 minutes, and 24 hours. 30uL of 5% formic acid in water was added to aliquot to halt cyclization. Samples were diluted 1:4 by removing 50uL of sample and adding 250uL water to allow for more sample runs for analysis. 10uL injections were run on the Xevo Tandem Quadrupole Mass using multiple reaction monitoring (MRM), monitoring for payload. Scanned transitions for resiquimod are 314.40 → 251.4; transitions for dexamethasone are 373.3 → 147.0, 237.1, and 337.1; transitions for doxorubicin are 545.2 → 332.3, 361.8, and 390.3. All samples were diluted 1:1 with an internal standard of albendazole, with transitions of 265.8 → 192.1 and 234.1.

### **10.9 Ramos Blue Cell Stimulation Assay**

A 3-fold dilution of each ADC and mAb was performed in the first wells of each row to prepare for the dosing of cells, this was done in 100% PBS. The dilution into the wells was 1:10, therefore the initial concentration of each ADC and mAb was 0.90mg/mL and 0.30mg/mL. Ramos blue cells (InvivoGen, cat# rms-sp) were cultured using high glucose IMDM media supplied with 10% fetal bovine serum according to the manufacturer guidelines. The media was supplemented with 50ug/mL penicillin, 50ug/mL streptomycin, 100ug/mL normocin, and 500ug/mL zeomycin to prevent bacterial contamination. The

cells were treated with Trypan Blue and the cell density and viability were calculated using a Countess Cell Counter and the proper volume of cells was removed to have a final seeding density of  $1.0 \times 10^6$  cells/mL per well after dilution with ADCs. Human serum was added to suspended cells before adding to the wells for a final volume of cells that consisted of 10% human serum. 135uL of cell suspension was added to every well in a 96-well plate along with 15uL of the corresponding ADC concentration (1:10 dilution of ADC), each done in triplicate. After 4 days of incubating at 37°C with 5% CO<sub>2</sub>, the plate was centrifuged at 1990rpm for 10 minutes and the 40uL of supernatant was added to 160uL of Quanti-Blue solution. The Quanti-Blue solution was prepared by adding 200uL of QB reagent (InvivoGen cat# rep-qbs) and 200uL of QB buffer to 19.6mL of water. The resulting solution was vortexed and incubated at room temperature for ten minutes. The QB reaction plate was incubated at 37°C for 4 hours and 24 hours. The plate was read at both 4 hours and 24 hours using a plate reader at a wavelength of 630 nm to determine the amount of SEAP production.

### **10.10 THP-1 Monocyte Suppression ADC Screen**

A 5-fold dilution of each ADC and mAb was performed in the first wells of each row to prepare for the dosing of cells, this was done in 100% PBS. The dilution into the wells was 1:10, therefore the initial concentration of each ADC and mAb was 0.30mg/mL and 0.06mg/mL. THP-1 Dual Cells (InvivoGen, cat# thpd-nfis) were cultured using high glucose RPMI media supplied with 10% fetal bovine serum and 25mM HEPES according to the manufacturer guidelines. The media was supplemented with 50ug/mL penicillin, 50ug/mL streptomycin, 100 ug/mL normocin, 500ug/mL blasticidin, and 500ug/mL zeomycin to prevent bacterial contamination. The cells were treated with Trypan Blue and

the cell density and viability were calculated using a Countess Cell Counter and the proper volume of cells was removed to have a final seeding density of  $0.2 \times 10^6$  cells/mL per well after dilution with ADCs. Human serum was added to suspended cells before adding to the wells for a final volume of cells that consisted of 10% human serum. 120uL of cell suspension was added to every well in a 96-well plate along with 15uL of the corresponding ADC concentration (1:10 dilution of ADC), each done in triplicate. Plates were incubated at 37°C with 5% CO<sub>2</sub> for 4 hours. Lipopolysaccharides (LPS) isolated from *E. coli*, was diluted down to 10ng/mL in PBS and then 15uL was added to each well (1:10 dilution, final 1ng/mL LPS concentration). After 16 hours of incubating at 37°C with 5% CO<sub>2</sub>, the plate was centrifuged at 1990rpm for 10 minutes and the 40uL of supernatant was added to 160uL of Quanti-Blue solution. The Quanti-Blue solution was prepared by adding 200uL of QB reagent (InVivogen cat# rep-qbs) and 200uL of QB buffer to 19.6mL of water. The resulting solution was vortexed and incubated at room temperature for ten minutes. The QB reaction plate was incubated at 37°C for 4 hours and 24 hours. The plate was read at both 4 hours and 24 hours using a plate reader at a wavelength of 630 nm to determine the amount of SEAP production. Luciferase production was quantified by adding 20uL of the supernatant to 50uL of Quanti-Luc solution in an opaque bottom 96-well plate and immediately analyzing luminescence at 100ms and 500ms to determine IRF pathway activation. Quanti-Luc solution was made by manufacturer guidelines, 25mL of sterile water added to purchased mix, aliquoted and froze till use.

Identical procedure was implemented for the anti-TNF $\alpha$  ADC dose response expect for initial ADC and mAb dilutions. 3-fold dilution was conducted to evaluate final

concentrations incubated with cells of 30ug/mL, 10ug/ml, 3.3ug/mL, 1.1ug/mL, 0.36ug/mL.

Identical procedure was implemented to test anti-CD11a ADCs, anti-CD11a mAb, and anti-Her2 ADCs for suppression of TNF $\alpha$ . The only difference was the larger dose response at lower concentration and an incubation time of 24hours with ADCs and then 24hours after LPS stimulation. Supernatant was analyzed for TNF $\alpha$  by ELISE. Experiment was designed and conducted by Siteng Fang.

### 10.11 Normal Analytical UPLC-MS Method

Analytical characterization was performed using a Water Acquity H-Class UPLC<sup>®</sup> with TUV detector, FLR detector, and QDa mass spectrometer. Typically, 1 $\mu$ l injections were separated using an Acquity UPLC BEH C18 1.7  $\mu$ m column (2.1 x 50mm) at 80°C. Eluent was monitored by UV (220 and 254nm), fluorescence (ex. 488nm, em. 520nm) and mass spectrometry (150-1250 Da, ES+/ES-). Solvents for the mobile phase were water with 0.1% formic acid (solvent A) and acetonitrile (ACN) with 0.1% formic acid (solvent B). Flow rate was 0.8 ml/min. Gradient Used: Isocratic solvent B for 0.8 min (0-0.8min), then gradient from 10%-95% Solvent B over 4.2 min (0.8-4.5min), isocratic solvent B for 0.3 min (4.5-4.8min), then gradient from 95% solvent B over 0.1 min (4.8-4.9min), then isocratic solvent B for 0.1 min (4.9-5.0min) (*Table 1*).

*Table 1: Solvent Gradient of Normal UPLC-MS Method*

Time (min)	Flow Rate (ml/min)	%A	%B
Initial	0.80	90.0%	10.0%
0.80	0.80	90.0%	10.0%
4.50	0.80	10.0%	90.0%
4.80	0.80	10.0%	90.0%
4.90	0.80	90.0%	10.0%

## 10.12 Normal Analytical HPLC-MS Method

Analytical characterization of large (> 1250 Da) organic compounds was performed using a Waters Auto-purification system containing a 2545 binary gradient module, 2767 sample manager, 2998 UV/PDA detector, and SQD2 mass spectrometer. Typically, 1 $\mu$ l injections were separated using an XBridge BEH C18 5 $\mu$ m (4.6 x 100 mm) column at 80°C. Eluent was monitored by UV (210-600nm), and mass spectrometry (150-1800 Da, ES+/ES-). Solvents for the mobile phase were water with 0.05% formic acid (solvent A) and acetonitrile (ACN) with 0.05% formic acid (solvent B). Flow rate was 2.00 ml/min. Gradient Used: Isocratic solvent B for 1.0 min (0-1.0 min), then gradient from 5% to 99% solvent B over 2.8 min (1.0-3.8min), then isocratic solvent B for 0.1 min (3.8-3.9min), then gradient from 99% to 5% solvent B for 0.1 min (3.9-4.0min), then isocratic solvent B for 1.0 min (4.0-5.0min) (*Table 2*).

*Table 2: Solvent Gradient for Normal Analytical HPLC-MS Method*

Time	Flow rate (mL/min)	%A	%B
Initial	2.00	95.0%	5.0%
1.00	2.00	95.0%	5.0%
3.80	2.00	1.0%	99.0%
3.90	2.00	1.0%	99.0%
4.00	2.00	95.0%	5.0%
5.00	2.00	95.0%	5.0%

## 10.13 Normal Preparative HPLC Method

General purification of organic compounds was performed using a Waters Auto-purification system containing a 2545 binary gradient module, 2767 sample manager, 2998

UV/PDA detector, and SQD2 mass spectrometer. Typically, 500µl injections were separated using an XBridge BEH C18 5 µm OBD (19 x 100 mm) prep column at room temperature. Eluent was monitored by UV (210-600nm), and mass spectrometry (150-2500 Da, ES+/ES-). Solvent for the mobile phase were water with 0.05% trifluoroacetic acid (solvent A) and acetonitrile (ACN) with 0.05% trifluoroacetic acid (solvent B). Flow rate was 20.0 ml/min. Gradient Used: Isocratic solvent B for 1.0 min (0-1.0min), then gradient from 15% to 95% solvent B over 7.0 min (1.0-8.0min), then isocratic solvent B for 0.5 min (8.0-8.5min), then gradient from 95% to 15% solvent B for 0.5 min (8.5-9.0min), then isocratic solvent B for 1.0 min (9.0-10.0min) (*Table 3*).

*Table 3: Solvent Gradient for Normal preparative HPLC Method*

Time	Flow rate (mL/min)	%A	%B
Initial	20.0	85.0%	15.0%
1.00	20.0	85.0%	15.0%
8.00	20.0	5.0%	95.0%
8.50	20.0	5.0%	95.0%
9.00	20.0	85.0%	15.0%
10.00	20.0	85.0%	15.0%

## 11. Supplemental Material

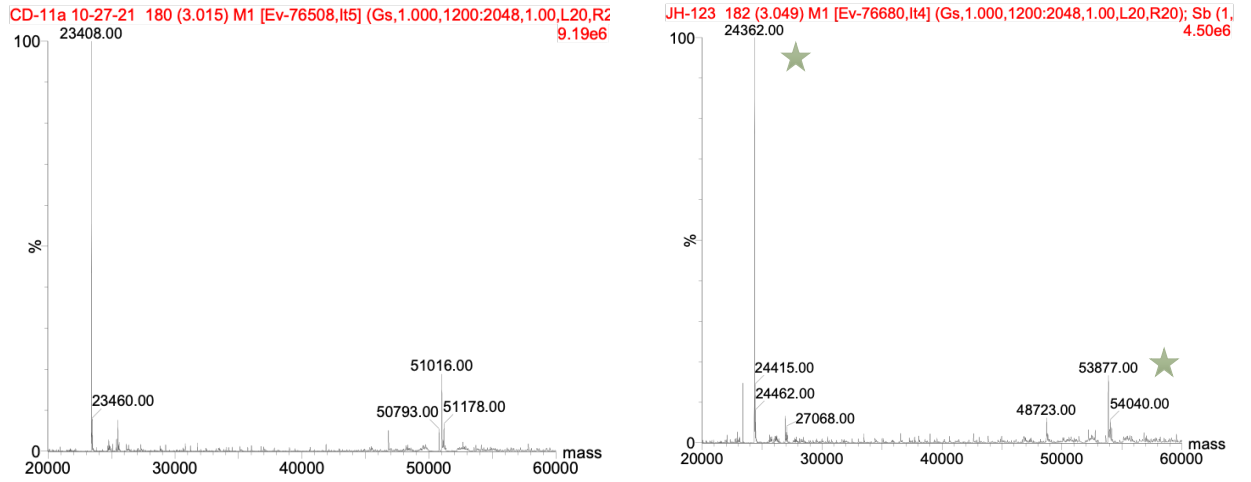


Figure S 1: anti-CD11a<sub>mpValCitGlyPro<sub>dex</sub></sub> mass spectrometry traces, linker-payload exact mass:

~953dalt

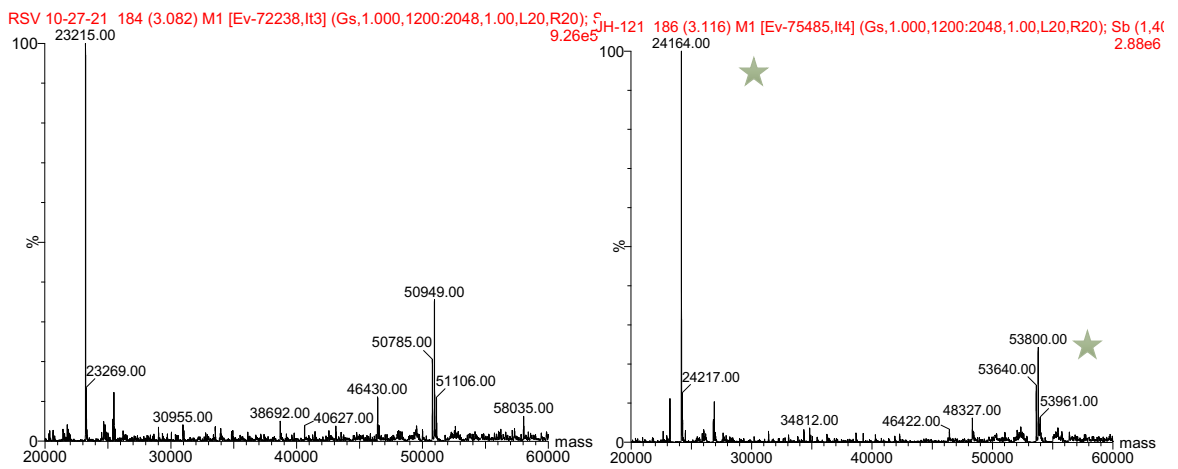


Figure S 2: anti-RSV<sub>mpValCitGlyPro<sub>dex</sub></sub> mass spectrometry traces, linker-payload exact mass:

~953dalt



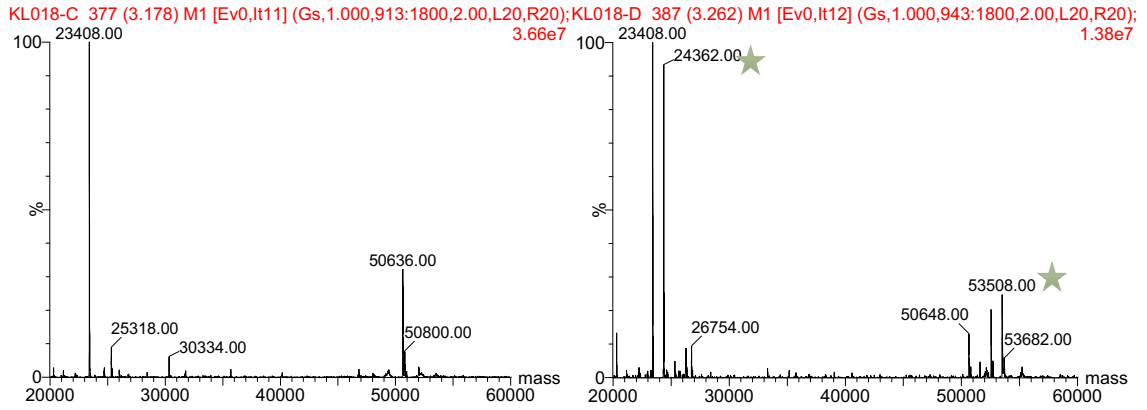


Figure S 3: anti-TNF $\alpha$  *\_mpValCitGlyPro\_dex* mass spectrometry traces, linker-payload exact mass:  
~953dalt

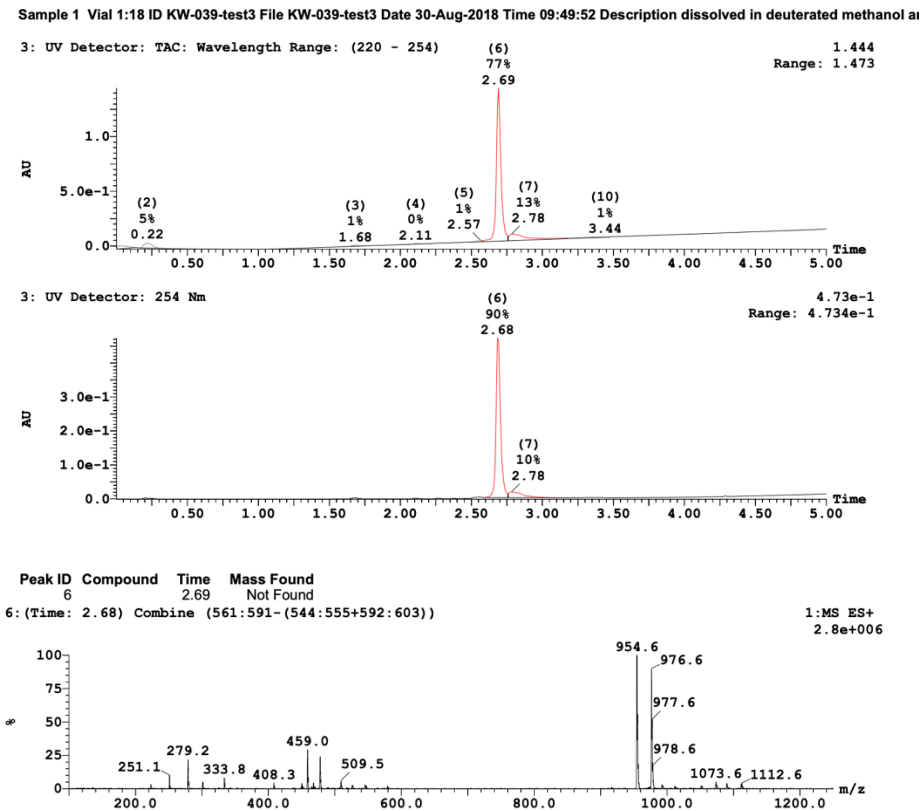
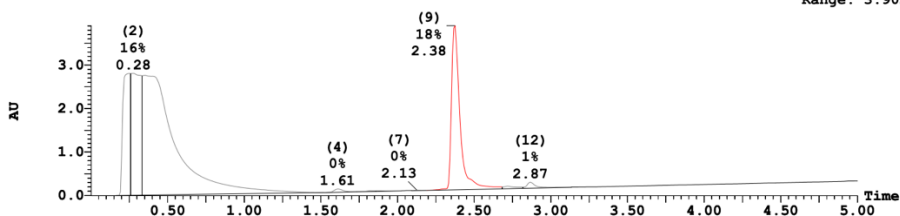


Figure S 4: LCMS Trace Characterization for *\_mpValCitGlyPro\_dex*

Sample 1 Vial 1:4 ID JH-060-1 File JH-060-1 Date 07-Nov-2020 Time 13:46:36 Description

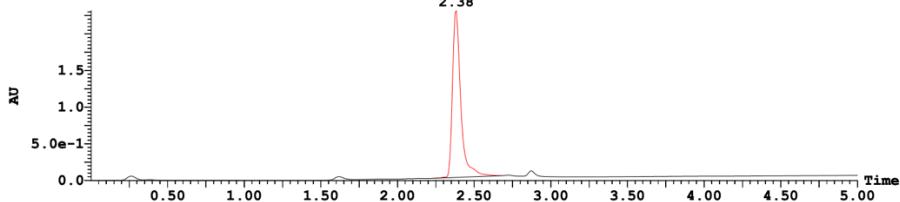
3: UV Detector: TAC: Wavelength Range: (220 - 254)

3.902  
Range: 3.902



3: UV Detector: 254 Nm

2.318  
Range: 2.319



Sample Report (continued):

Peak ID	Compound	Time	Mass Found
9		2.36	Not Found

9: (Time: 2.38) Combine (496:526-(467:478+576:586))

1:MS ES+  
1.0e+007

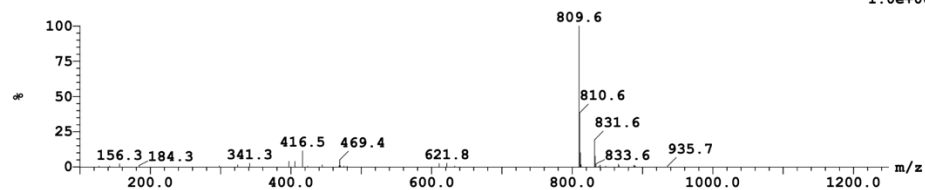
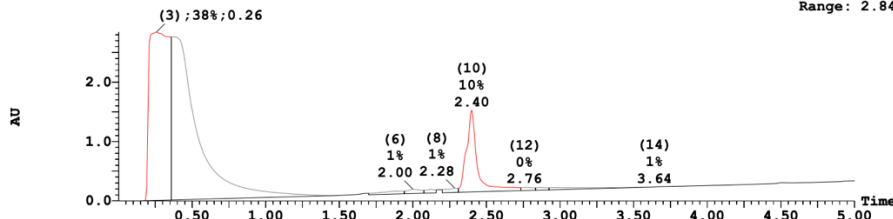


Figure S 5: LCMS Trace Characterization for alloc\_ValCitGlyPro\_resiquimod

Sample 1 Vial 1:4 ID JH-060-F File JH-060-F Date 12-Nov-2020 Time 12:20:34 Description

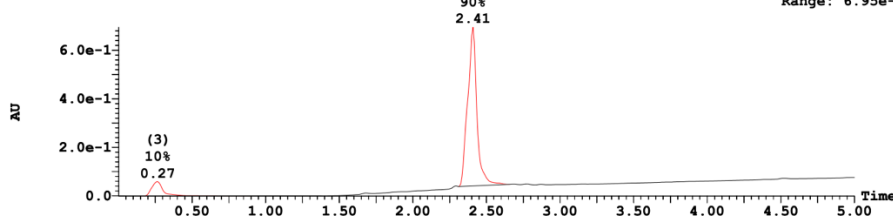
3: UV Detector: TAC: Wavelength Range: (220 - 254)

2.843  
Range: 2.843



3: UV Detector: 254 Nm

6.946e-1  
Range: 6.95e-1



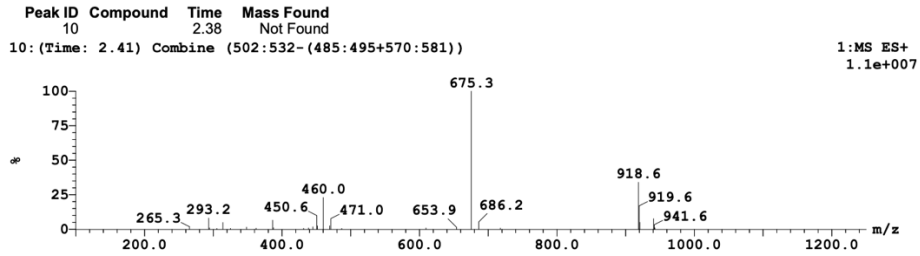


Figure S 6: LCMS Trace Characterization for mcValCitGlyPro\_resiquimod

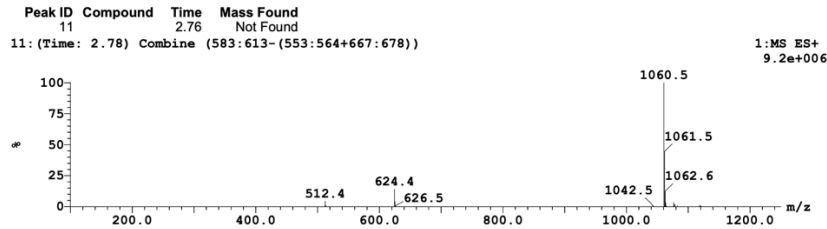
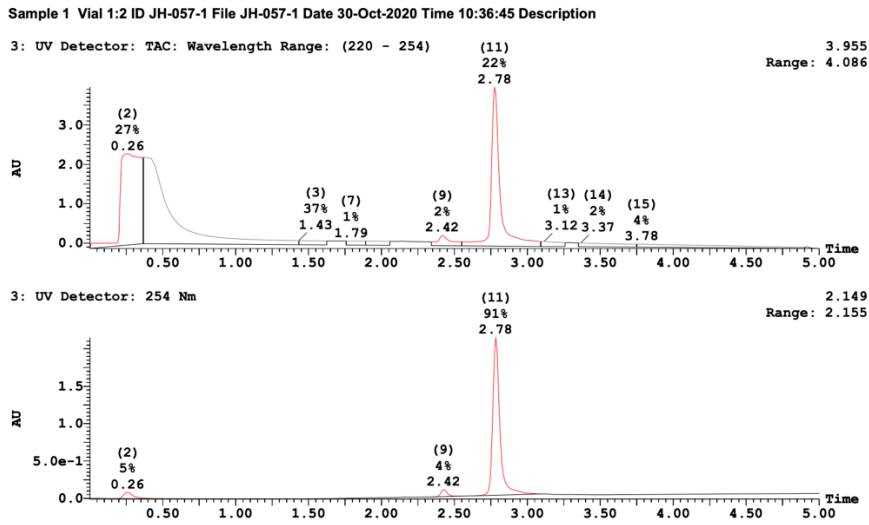
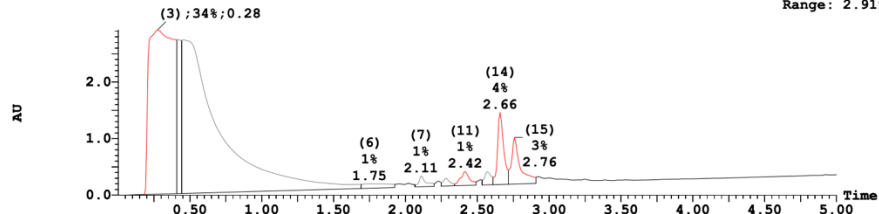


Figure S 7: LCMS Trace Characterization for alloc\_ValCitGlyPro\_doxorubicin

Sample 1 Vial 1:4 ID JH-057-F2 File JH-057-F2 Date 05-Nov-2020 Time 13:13:03 Description

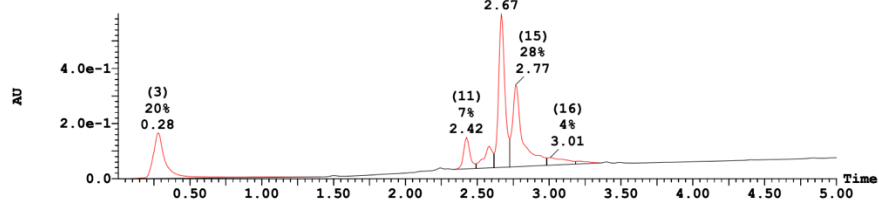
3: UV Detector: TAC: Wavelength Range: (220 - 254)

2.919  
Range: 2.919



3: UV Detector: 254 Nm

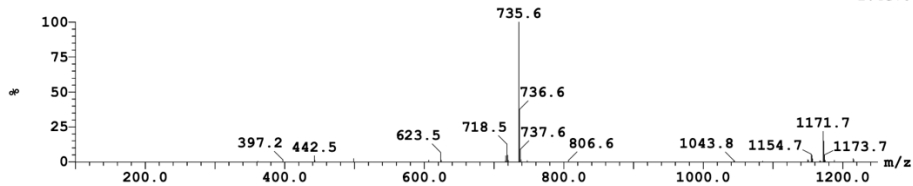
5.992e-1  
Range: 5.993e-1



Peak ID	Compound	Time	Mass Found
14		2.66	Not Found

14: (Time: 2.67) Combine (557:587- (551:562+585:596))

1:MS ES+  
1.4e+006



Peak ID	Compound	Time	Mass Found
15		2.73	Not Found

15: (Time: 2.77) Combine (579:609- (574:585+640:651))

1:MS ES+  
1.0e+006

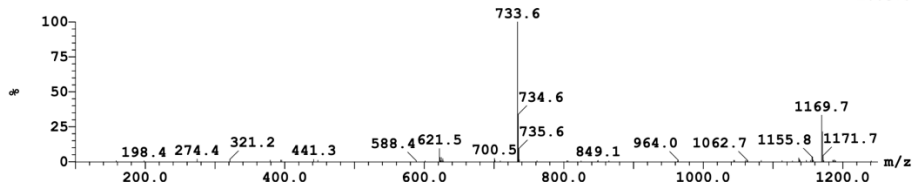
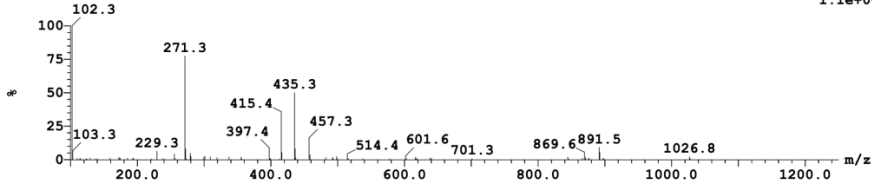
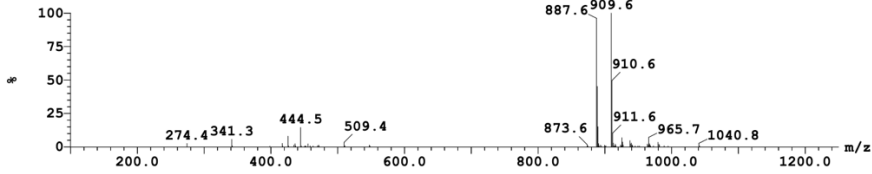


Figure S 8: LCMS Trace Characterization for mcValCitGlyPro\_doxorubicin

Peak ID Compound Time Mass Found  
 8 (Time: 2.94) Combine (616:646-(595:606+651:662)) 1:MS ES+  
 1.1e+006

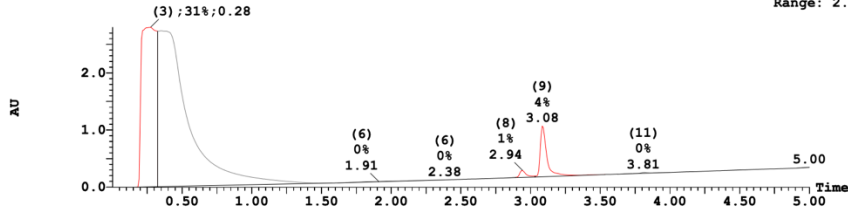


Peak ID Compound Time Mass Found  
 9 (Time: 3.09) Combine (648:678-(640:651+706:717)) 1:MS ES+  
 2.5e+006



Sample 1 Vial 1:8 ID JH-061-1 File JH-061-1 Date 19-Nov-2020 Time 12:31:54 Description

3: UV Detector: TAC: Wavelength Range: (220 - 254) 2.799  
 Range: 2.8



3: UV Detector: 254 Nm 5.117e-1  
 Range: 5.12e-1

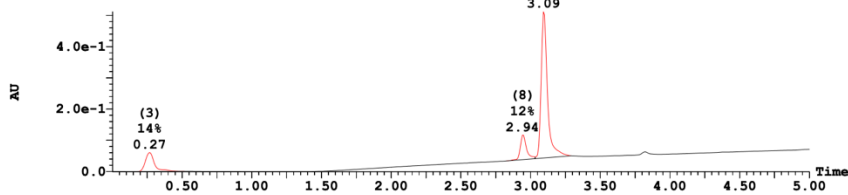
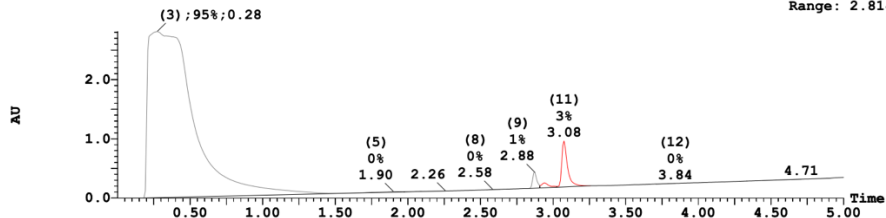


Figure S 9: LCMS Trace Characterization for alloc\_ValCitGlyPro\_dexamethasone

Sample 1 Vial 1:8 ID JH-062-F File JH-062-F Date 24-Nov-2020 Time 10:37:54 Description

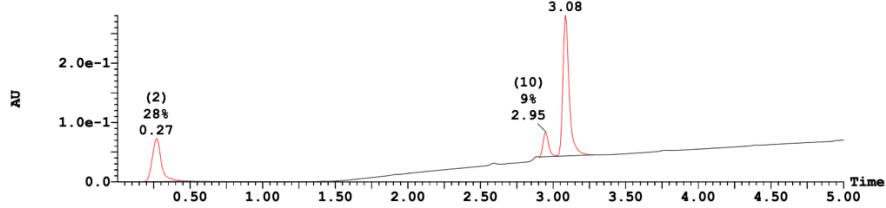
3: UV Detector: TAC: Wavelength Range: (220 - 254)

2.814  
Range: 2.814



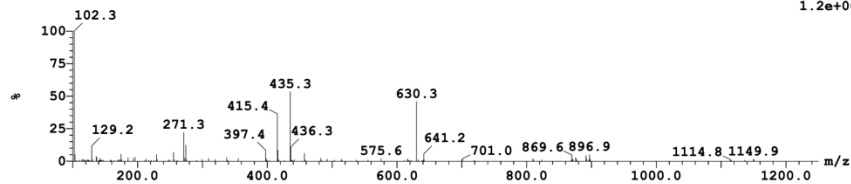
3: UV Detector: 254 Nm

2.809e-1  
Range: 2.809e-1



Peak ID Compound Time Mass Found  
10 (Time: 2.95) Combine (618:648-(612:622+649:660))

1:MS ES+  
1.2e+006



Peak ID Compound Time Mass Found  
11 (Time: 3.08) Combine (647:677-(638:649+704:715))

1:MS ES+  
2.5e+006

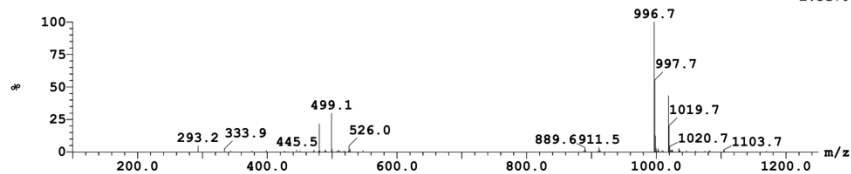


Figure S 10: LCMS Trace Characterization for mcValCitGlyPro\_dexamethasone

Table 4: List of ADCs, their DAR, concentration, and aggregation

ADC Name	DAR	Concentration (mg/mL)	Aggregation
Anti-CD11a_mpValCitGlyPro_dex	6.2	1.010	<5%
Anti-CD11a_mpValCitGlyPro_dex	7.7	0.800	<5%
Anti-Her2_mpValCitGlyPro_dex	5.7	0.700	<5%

Anti-Her2_mpValCitGly(D)Pro_dex	6.8	0.400	<5%
Anti-CD38_mpValCitGlyPro_dex	2.5	0.538	<5%
Anti-RSV_mpValCitGlyPro_dex	7.8	0.905	<5%
Anti-TNF $\alpha$ _mpValCitGlyPro_dex	4.5	0.928	<5%
Anti-MSR1_mpValCitGlyPro_dex	7.7	0.640	<5%
Anti-RSV_mcValCitGlyPro_resiquimod	7.9	1.010	<5%
Anti-CD38_mcValCitGlyPro_resiquimod	6.5	0.930	<5%

## 12. Acknowledgements

I would like to first and foremost, acknowledge my research professor and mentor Dr. L. Nathan Tumey, who has helped and guided me through two and a half years of research and personal development. My honors thesis committee members, Dr. Ming An and Dr. Christof Grewer, for teaching me inside the classroom and supporting me through my thesis. My research lab for helping me through my experiments and data analysis, while also being excellent friends outside the lab. Lastly, thank you to Binghamton University, Summer Scholars and Artists program, and the SUNY Research Foundation for funding, of which, this project would not have been possible.

### 13. References

- (1) Doronina, S. O.; Bovee, T. D.; Meyer, D. W.; Miyamoto, J. B.; Anderson, M. E.; Morris-Tilden, C. A.; Senter, P. D. Novel Peptide Linkers for Highly Potent Antibody-Auristatin Conjugate. *Bioconjugate Chemistry* **2008**, *19* (10), 1960–1963. <https://doi.org/10.1021/bc800289a>.
- (2) Bae, Y. H.; Park, K. Targeted Drug Delivery to Tumors: Myths, Reality and Possibility. *J Control Release* **2011**, *153* (3), 198–205. <https://doi.org/10.1016/j.jconrel.2011.06.001>.
- (3) Parslow, A. C.; Parakh, S.; Lee, F.-T.; Gan, H. K.; Scott, A. M. Antibody-Drug Conjugates for Cancer Therapy. *Biomedicines* **2016**, *4* (3), 14. <https://doi.org/10.3390/biomedicines4030014>.
- (4) Dean, A. Q.; Luo, S.; Twomey, J. D.; Zhang, B. Targeting Cancer with Antibody-Drug Conjugates: Promises and Challenges. *mAbs*. Bellwether Publishing, Ltd. 2021. <https://doi.org/10.1080/19420862.2021.1951427>.
- (5) Tsuchikama, K.; An, Z. Antibody-Drug Conjugates: Recent Advances in Conjugation and Linker Chemistries. *Protein & Cell* **2018**, *9* (1), 33–46. <https://doi.org/10.1007/s13238-016-0323-0>.
- (6) Bargh, J. D.; Walsh, S. J.; Isidro-Llobet, A.; Omarjee, S.; Carroll, J. S.; Spring, D. R. Sulfatase-Cleavable Linkers for Antibody-Drug Conjugates. *Chemical Science* **2020**, *11* (9), 2375–2380. <https://doi.org/10.1039/c9sc06410a>.
- (7) Miller, J. T.; Vitro, C. N.; Fang, S.; Benjamin, S. R.; Tumey, L. N. Enzyme-Agnostic Lysosomal Screen Identifies New Legumain-Cleavable ADC



- Linkers. *Bioconjugate Chemistry* **2021**, *32* (4), 842–858.  
<https://doi.org/10.1021/acs.bioconjchem.1c00124>.
- (8) Jeffrey, S. C.; Nguyen, M. T.; Moser, R. F.; Meyer, D. L.; Miyamoto, J. B.; Senter, P. D. Minor Groove Binder Antibody Conjugates Employing a Water Soluble  $\alpha$ -Glucuronide Linker. *Bioorganic and Medicinal Chemistry Letters* **2007**, *17* (8), 2278–2280.  
<https://doi.org/10.1016/j.bmcl.2007.01.071>.
- (9) Kern, J. C.; Cancilla, M.; Dooney, D.; Kwasnjuk, K.; Zhang, R.; Beaumont, M.; Figueroa, I.; Hsieh, S. C.; Liang, L.; Tomazela, D.; Zhang, J.; Brandish, P. E.; Palmieri, A.; Stivers, P.; Cheng, M.; Feng, G.; Geda, P.; Shah, S.; Beck, A.; Bresson, D.; Firdos, J.; Gately, D.; Knudsen, N.; Manibusan, A.; Schultz, P. G.; Sun, Y.; Garbaccio, R. M. Discovery of Pyrophosphate Diesters as Tunable, Soluble, and Bioorthogonal Linkers for Site-Specific Antibody-Drug Conjugates. *J Am Chem Soc* **2016**, *138* (4), 1430–1445.  
<https://doi.org/10.1021/jacs.5b12547>.
- (10) Lerchen, H. G.; Stelte-Ludwig, B.; Sommer, A.; Berndt, S.; Rebstock, A. S.; Johannes, S.; Mahlert, C.; Greven, S.; Dietz, L.; Jörißen, H. Tailored Linker Chemistries for the Efficient and Selective Activation of ADCs with KSPi Payloads. *Bioconjug Chem* **2020**, *31* (8), 1893–1898.  
<https://doi.org/10.1021/acs.bioconjchem.0c00357>.
- (11) Carl, P. L.; Chakravarty, P. K.; Katzenellenbogen, J. A. A Novel Connector Linkage Applicable in Prodrug Design. *Journal of Medicinal Chemistry* **1981**, *24* (5), 479–480. <https://doi.org/10.1021/jm00137a001>.

- (12) Dubowchik, G. M.; Firestone, R. A. Cathepsin B-Sensitive Dipeptide Prodrugs. 1. A Model Study of Structural Requirements for Efficient Release of Doxorubicin. *Bioorganic and Medicinal Chemistry Letters* **1998**, *8* (23), 3341–3346. [https://doi.org/10.1016/S0960-894X\(98\)00609-X](https://doi.org/10.1016/S0960-894X(98)00609-X).
- (13) Dubowchik, G. M.; Firestone, R. A.; Padilla, L.; Willner, D.; Hofstead, S. J.; Mosure, K.; Knipe, J. O.; Lasch, S. J.; Trail, P. A. Cathepsin B-Labile Dipeptide Linkers for Lysosomal Release of Doxorubicin from Internalizing Immunoconjugates: Model Studies of Enzymatic Drug Release and Antigen-Specific in Vitro Anticancer Activity. *Bioconjugate Chemistry* **2002**, *13* (4), 855–869. <https://doi.org/10.1021/bc025536j>.
- (14) Dal Corso, A.; Borlandelli, V.; Corno, C.; Perego, P.; Belvisi, L.; Pignataro, L.; Gennari, C. Fast Cyclization of a Proline-Derived Self-Immolative Spacer Improves the Efficacy of Carbamate Prodrugs. *Angewandte Chemie* **2020**, *132* (10), 4205–4210. <https://doi.org/10.1002/ange.201916394>.
- (15) Liu, T.; Zhang, L.; Joo, D.; Sun, S. C. NF-KB Signaling in Inflammation. *Signal Transduction and Targeted Therapy*. Springer Nature 2017. <https://doi.org/10.1038/sigtrans.2017.23>.
- (16) Monaco, C.; Nanchahal, J.; Taylor, P.; Feldmann, M. Anti-TNF Therapy: Past, Present and Future. *Int Immunol* **2015**, *27* (1), 55–62. <https://doi.org/10.1093/intimm/dxu102>.
- (17) Udalova, I.; Monaco, C.; Nanchahal, J.; Feldmann, M. Anti-TNF Therapy. **2016**. <https://doi.org/10.1128/microbiolspec.MCHD-0022-2015>.

- (18) Kolakowski, R. v; Haelsig, K. T.; Emmerton, K. K.; Leiske, C. I.; Miyamoto, J. B.; Cochran, J. H.; Lyon, R. P.; Senter, P. D.; Jeffrey, S. C. The Methylene Alkoxy Carbamate Self-Immolative Unit: Utilization for the Targeted Delivery of Alcohol-Containing Payloads with Antibody???Drug Conjugates. *Angewandte Chemie - International Edition* **2016**, *55* (28), 7948–7951. <https://doi.org/10.1002/anie.201601506>.
- (19) Elgersma, R. C.; Coumans, R. G. E.; Huijbregts, T.; Menge, W. M. P. B.; Joosten, J. A. F.; Spijker, H. J.; de Groot, F. M. H.; van der Lee, M. M. C.; Ubink, R.; van den Dobbelsteen, D. J.; Egging, D. F.; Dokter, W. H. A.; Verheijden, G. F. M.; Lemmens, J. M.; Timmers, C. M.; Beusker, P. H. Design, Synthesis, and Evaluation of Linker-Duocarmycin Payloads: Toward Selection of HER2-Targeting Antibody-Drug Conjugate SYD985. *Molecular Pharmaceutics* **2015**, *12* (6), 1813–1835. <https://doi.org/10.1021/mp500781a>.
- (20) Agnello, S.; Brand, M.; Chellat, M. F.; Gazzola, S.; Riedl, R. Eine Strukturelle Evaluierung Medizinalchemischer Strategien Gegen Wirkstoffresistenzen. *Angewandte Chemie* **2019**, *131* (11), 3336–3383. <https://doi.org/10.1002/ange.201802416>.
- (21) Knipe, A. C.; Stirling, C. J. M. *Elimination-Addition. Part XV.l Rates of Reactions of  $\alpha$ -Bromoalkyl *p*-Tolyl Sulphides with Alkoxides : The Role of Neighbouring Group Participation by Sulphur and the Involvement of Lon-Pair Equilibria*; 1968; Vol. 808.

- (22) Adjuvant Potential of Resiquimod with Inactivated Newcastle Disease Vaccine and Its Mechanism of Action in Chicken \_ Elsevier Enhanced Reader.
- (23) Rodell, C. B.; Arlauckas, S. P.; Cuccarese, M. F.; Garriss, C. S.; Li, R.; Ahmed, M. S.; Kohler, R. H.; Pittet, M. J.; Weissleder, R.; Biomed Eng, N. *TLR7/8-Agonist-Loaded Nanoparticles Promote the Polarization of Tumour-Associated Macrophages to Enhance Cancer Immunotherapy HHS Public Access Author Manuscript.*
- (24) Novakovic, B. J. Immunotoxin-a New Treatment Option in Patients with Relapsed and Refractory Hodgkin Lymphoma. *Radiology and Oncology* **2015**, *49* (4), 315–319.